Molecular Therapy
Oncology
Original Article

# Mediation of antitumor activity by AZD4820 oncolytic vaccinia virus encoding IL-12

Cheyne Kurokawa,[1] Sonia Agrawal,[2] Abhisek Mitra,[3] Elena Galvani,[4] Shannon Burke,[4] Ankita Varshine,[3] Raymond Rothstein,[3] Kevin Schifferli,[3] Noel R. Monks,[3] Johann Foloppe,[5] Nathalie Silvestre,[5] Eric Quemeneur,[5] Christelle Demeusoit,[5] Patricia Kleinpeter,[5] Puja Sapra,[3] Carl Barrett,[2] Scott A. Hammond,[3] Elizabeth J. Kelly,[6] Jason Laliberte,[1] Nicholas M. Durham,[2] Michael Oberst,[3] and Maria A.S. Broggi[2]

[1]Virology and Vaccine Discovery, BioPharmaceuticals R&D, AstraZeneca, Gaithersburg, MD, USA; [2]Translational Medicine, Oncology R&D, AstraZeneca, Gaithersburg, MD, USA; [3]Biologics Engineering and Targeted Delivery, Oncology R&D, AstraZeneca, Gaithersburg, MD, USA; [4]Biologics Engineering and Targeted Delivery, Oncology R&D, AstraZeneca, Cambridge, UK; [5]Department of Research, Transgene SA, Illkirch-Graffenstaden, France; [6]Clinical Virology, BioPharmaceuticals R&D, AstraZeneca, Gaithersburg, MD, USA

**Oncolytic viruses are engineered to selectively kill tumor cells and have demonstrated promising results in early-phase clinical trials. To further modulate the innate and adaptive immune system, we generated AZD4820, a vaccinia virus engineered to express interleukin-12 (IL-12), a potent cytokine involved in the activation of natural killer (NK) and T cells and the reprogramming of the tumor immune microenvironment. Testing in cultured human tumor cell lines demonstrated broad *in vitro* oncolytic activity and IL-12 transgene expression. A surrogate virus expressing murine IL-12 demonstrated antitumor activity in both MC38 and CT26 mouse syngeneic tumor models that responded poorly to immune checkpoint inhibition. In both models, AZD4820 significantly upregulated interferon-gamma (IFN-γ) relative to control mice treated with oncolytic vaccinia virus (VACV)-luciferase. In the CT26 study, 6 of 10 mice had a complete response after treatment with AZD4820 murine surrogate, whereas control VACV-luciferase–treated mice had 0 of 10 complete responders. AZD4820 treatment combined with anti–PD-L1 blocking antibody augmented tumor-specific T cell immunity relative to monotherapies. These findings suggest that vaccinia virus delivery of IL-12, combined with immune checkpoint blockade, elicits antitumor immunity in tumors that respond poorly to immune checkpoint inhibitors.**

## INTRODUCTION

Numerous oncolytic virus (OV) platforms are undergoing clinical evaluation in solid-tumor indications. Therapeutic responses in early-stage clinical trials have been achieved for some, demonstrating biological activity in indications such as melanoma, hepatocellular carcinoma (HCC), colorectal cancer (CRC), ovarian cancer, glioblastoma, and breast cancer.[1–5] The OV talimogene laherparepvec (T-VEC; Imlygic), an oncolytic herpesvirus engineered to express granulocyte-macrophage-colony-stimulating factor (GM-CSF), has been approved by the US Food and Drug Administration for the local (intratumoral) treatment of unresectable cutaneous, subcutaneous, and nodal lesions in patients with melanoma recurring after initial surgery.[6] Other OV platforms in clinical development include engineered adenovirus, Newcastle disease virus, measles virus, vesicular stomatitis virus, poliovirus, coxsackie virus, parvovirus, retrovirus, reovirus, and vaccinia virus.[7] In most trials, oncolytic activity alone was not sufficient for clinical benefit, whereas arming herpesvirus (T-VEC) and vaccinia virus (pexastimogene devacirepvec [Pexa-Vec]; JX-594, Wyeth) with GM-CSF improved antitumor efficacy.[6,8]

To build on the early success of OVs armed with cytokines, we developed AZD4820, an engineered oncolytic vaccinia virus (VACV) in the Copenhagen strain. VACVs are enveloped, double-stranded DNA poxviruses with the capacity to encode large transgenes.[9] AZD4820 contains deletions in viral thymidine kinase (TK) and ribonucleotide reductase (RR) large subunit (RRM1) that enhance tumor-specific replication.[9] It encodes a human interleukin-12 (IL-12) fusion protein transgene consisting of the p40 and p35 subunits of IL-12 covalently linked by a glycine-serine linker. The transgene is inserted into the J2R (viral TK) locus and is controlled by the late virus promoter pF17R to limit IL-12 production to cells in which AZD4820 is actively replicating, such as tumor cells. Confining IL-12 production to tumors has the goal of maximizing IL-12 antitumor activity while limiting potential systemic toxicities.

AZD4820 has other VACV characteristics that make it an attractive agent for anticancer therapy. VACVs have evolved in mammalian species, including humans, to disseminate within the host through the formation of two distinct infectious virions: intracellular mature virus and extracellular enveloped virus.[10,11] This characteristic has

Received 17 March 2023; accepted 22 November 2023;
https://doi.org/10.1016/j.omton.2023.200758.

**Correspondence:** Michael Oberst, Biologics Engineering and Targeted Delivery, Oncology R&D, AstraZeneca, Gaithersburg, MD 20878, USA.
**E-mail:** michael.oberst@astrazeneca.com
**Correspondence:** Maria A.S. Broggi, Translational Medicine, Oncology R&D, AstraZeneca, Gaithersburg, MD 20878, USA.
**E-mail:** maria.broggi@astrazeneca.com

resulted in adaptations that allow the virus to circumvent complement-mediated clearance and to minimize anti-VACV neutralizing antibodies.[12,13] VACV is a human pathogen and has evolved to evade immune detection by various means, including through the expression of virus proteins that evade interferon (IFN)-mediated antivirus defense.[14] Numerous live, attenuated strains of VACV have been generated in the campaign to eradicate smallpox, providing an important precedent for the safety and tolerability of VACV-based vaccines.[15] The VACV genome can also be modified further to increase tumor cell–specific replication, such as in AZD4820, where deletion of the vaccinia TK and RR genes limits virus replication to cells that express high levels of these enzymes, such as tumor cells.[9] These characteristics have allowed vaccine-derived VACV to become an attractive anticancer OV platform that is being tested in multiple clinical trials.

In tumors, it is believed that the oncolysis of cancer cells by VACV leads to an immunogenic cell death that releases pathogen-associated molecular patterns from virus and danger-associated molecular patterns from dying cancer cells. These may directly activate dendritic cell (DC) cross-presentation of tumor-associated antigens to induce antitumor T cell immunity.[16,17] This property of engineered VACV makes it an immunogenic agent capable of eliciting *in situ* vaccination against tumor neo-epitopes that may lead to an antitumor T cell response and immunological memory.[18,19] The expression of human IL-12 by replicating AZD4820 in human tumors may potentiate an antitumor immune response by engaging both innate and adaptive antitumor immunity.[20–22] The main IL-12 immunomodulating functions are (1) induction of T helper 1 differentiation of helper CD4 T cells and inhibition of CD4 $FoxP3^+$ regulatory T cell differentiation; (2) enhancement of T and natural killer (NK) cell cytotoxic activities; (3) inhibition and reprogramming of myeloid immunosuppressive cells, such as tumor-associated macrophages and myeloid-derived suppressor cells; and (4) enhancement of antigen presentation by DCs. Collectively, these activities facilitate a robust antitumor immune response. However, systemic IL-12 therapy at efficacious doses is limited by serious immune-related adverse events.[23] Therefore, modalities that localize the delivery of IL-12 to the tumor microenvironment (TME), such as through expression by OVs, are needed to enable the clinical success of IL-12 while minimizing systemic toxicities.

Immune checkpoint inhibitors (ICIs) targeting programmed cell death-1 (PD-1) and its ligand (PD-L1) or cytotoxic T lymphocyte–associated protein 4 (CTLA-4) have demonstrated success in the clinic as monotherapies or combination therapies,[24] but disease does not respond in all patients. Combining OVs with ICIs has demonstrated promising results in preclinical studies and in early-phase clinical trials.[25] A recent study demonstrated that treatment with several OVs, such as VACV and measles virus, can attract T cells to tumors and sensitize them to anti-PD-L1 or anti-PD-1 therapy,[26,27] suggesting that OVs provide a unique combination opportunity with ICIs.

In this study, we describe the generation and characterization of AZD4820. We evaluated the oncolytic activity of VACV in 47 primary patient-derived xenograft (PDX) models and found antitumor activity across eight of nine tumor indications. AZD4820 replicated and expressed IL-12 in fresh tumor slice cultures and primary dissociated tumor cell cultures representing multiple tumor types. We also evaluated the antitumor activity of AZD4820 in syngeneic rat and murine tumor models. AZD4820 generated a tumor-specific immune response that was amplified when combined with PD-L1 blockade in a murine tumor model that was poorly responsive to anti-PD-L1 therapy.

## RESULTS

### Efficacy of oncolytic VACV platform in multiple tumor types

To evaluate the antitumor activity of the oncolytic VACV platform, a TK- and RR-deleted VACV (Copenhagen strain) expressing firefly luciferase (VACV-LUC) was tested in 47 PDX tumor models representing bladder (n = 5), CRC (n = 7), head and neck squamous cell (HNSCC) (n = 7), HCC (n = 1), melanoma (n = 7), Merkel cell (n = 2), non-small cell lung (NSCLC) (n = 8), ovarian (n = 4), and small-cell lung (n = 6) cancers (Table S1). A single tumor from each PDX model was treated with three weekly doses of $10^7$ plaque-forming units (PFUs) of VACV-LUC by intravenous administration and compared to a vehicle-treated control tumor (Figure 1A). The best overall response (BOR) was determined by comparing tumor volume changes relative to tumor volume at the start of VACV-LUC treatment. Responses were considered evaluable in VACV-LUC-treated tumors only if the corresponding untreated control tumor showed progressive growth. Oncolytic VACV demonstrated antitumor activity (disease stabilization [DS], partial response [PR], or complete response [CR]) in 35 of 47 PDX models across multiple tumor indications (Figures 1B and S1; Table 1).

To evaluate VACV replication kinetics, virus replication was measured in tumor tissue 48 h after the first and third doses. Infectious virus was recovered from all of the tumor models and demonstrated a significant increase in virus replication between the first and third doses ($p = 0.0079$), strongly suggesting the accumulation and replication of VACV in treated tumors (Figure 1C). A comparison of BOR with VACV-LUC replication at these time points showed no correlation between virus replication and response (Figure S2), suggesting that the levels of virus replication measured at these time points did not predict antitumor activity.

Gene expression changes were also evaluated following treatment with VACV-LUC. RNA was isolated from the tumor and analyzed by RNA sequencing. Mouse-specific sequencing reads were analyzed to examine host transcriptomic changes within the TME. Although NOD/SCID mice lack T and B cells, they support the development of other innate immune cells, such as neutrophils, monocytes, NK cells, DCs, and macrophages, although the latter three contain functional deficits.[28,29] RNA-sequencing analysis revealed an increased expression of IL-12 receptor subunits IL-12rb1 and IL-12rb2, which are expressed on NK and T cells and can activate these leukocytes upon IL-12 binding. Expression of the IL-12 receptor subunits were

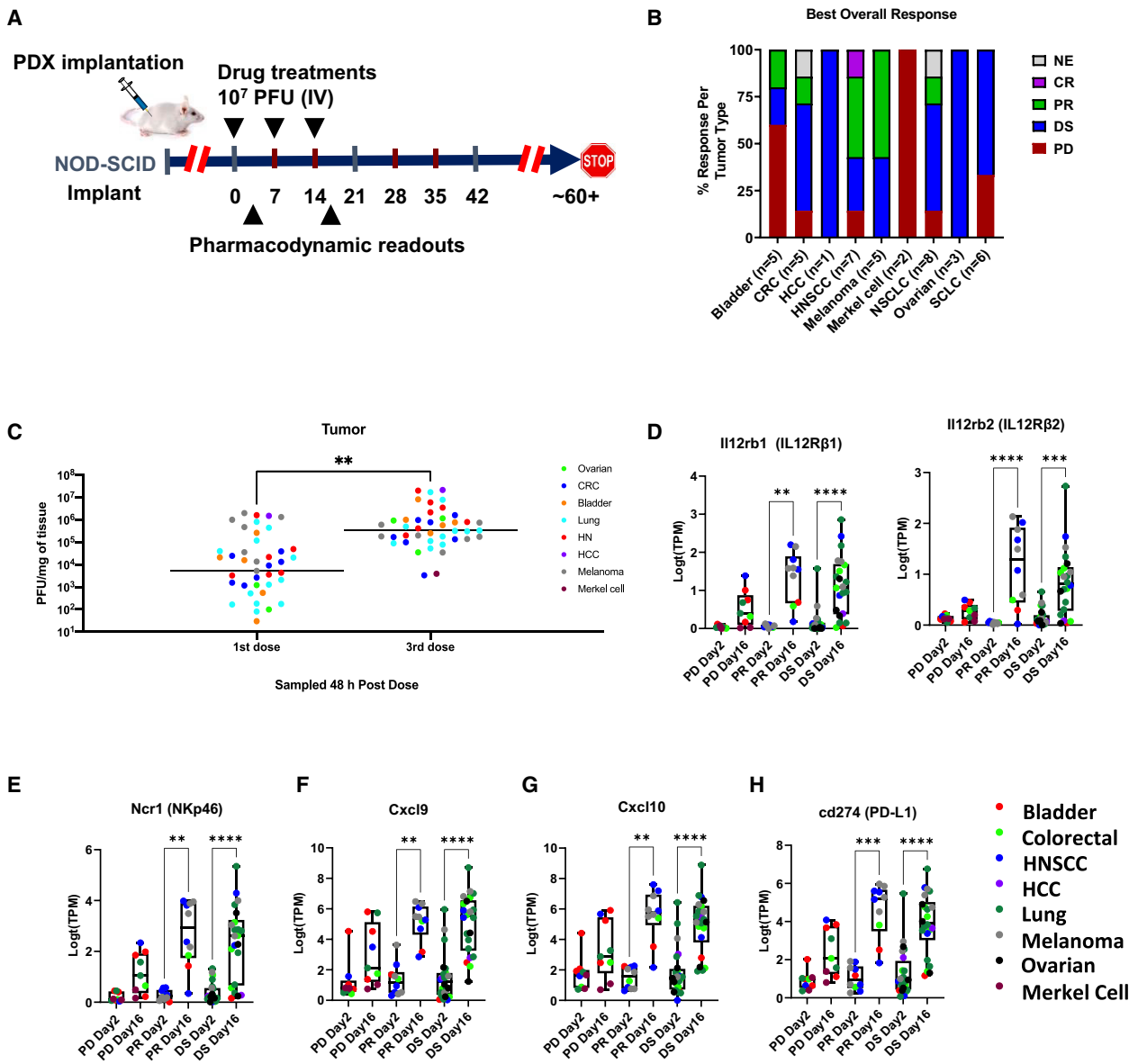


**Figure 1. Activity of VACV-LUC virus in mice engrafted with human PDX tumors**

(A) Determination of the antitumor activity of VACV-LUC virus against human PDX tumors. (B) BOR pattern for VACV-LUC-treated mice engrafted with different tumor types as indicated. (C) Recovery of virus from engrafted tumors at 48 h after the first or third dose of VACV-LUC as determined by virus plaque assay. **p = 0.0095, 2-tailed, paired Student t test. (D–H) At 48 h after the first or third dose of VACV-LUC, expression of mouse RNA transcripts according to response pattern for (D) IL-12 receptor β1 and β2, (E) NKp46, (F) Cxcl9, (G) Cxcl10, and (H) PD-L1. *p ≤ 0.05; **p ≤ 0.01; ***p ≤ 0.001; ****p ≤ 0.0001 by 1-way ANOVA with Kruskal-Wallis test for multiple comparisons. Bar, median; boxes range from 25th to 75th percentile; whiskers extend to lowest and highest values. HN, head and neck squamous cell carcinoma; IV, intravenous.

increased at later (day 16) versus earlier (day 2) treatment time points (Figure 1D). We also observed an increase in an NK cell–specific marker (*NKp46*), lymphoid recruiting chemokines *cxcl9* and *cxcl10*, and *cd274* (PD-L1) 2 days after the third dose (day 16) and at 2 days after the first dose (day 2) (Figures 1E–1H). These results suggest that VACV infection increases inflammation and NK cell recruitment within the TME and results in the engagement of compensatory negative feedback pathways such as PD-1/PD-L1. Notably, the magnitude of transcript increases was greater in models demonstrating PR or DS than in those showing PD.

### Generation of AZD4820 and oncolytic activity

Motivated by the results of oncolytic VACV activity observed across multiple tumor types, we next sought to arm VACV in a way that

**Table 1. Antitumor activity of VACV-LUC**

| Model | Tumor type | BOR |
|---|---|---|
| BL5001 | Bladder | PD |
| BL5002 | Bladder | PR |
| BL5003 | Bladder | PD |
| BL5007 | Bladder | DS |
| BL5422 | Bladder | PD |
| CR5027 | CRC | DS |
| CR5028 | CRC | DS |
| CR5030 | CRC | PD |
| CR5052 | CRC | DS |
| CR5063 | CRC | PR |
| CR5085 | CRC | NE |
| CR5087 | CRC | DS |
| LI5133 | HCC | DS |
| HN5110 | HNSSC | PD |
| HN5111 | HNSSC | CR |
| HN5113 | HNSSC | PR |
| HN5116 | HNSSC | PR |
| HN5120 | HNSSC | DS |
| HN5125 | HNSSC | DS |
| HN5126 | HNSSC | PR |
| ME11977 | Melanoma | DS |
| ME12209 | Melanoma | PR |
| ME12220 | Melanoma | PR |
| ME13983 | Melanoma | PR |
| ME14000 | Melanoma | PR |
| ME14004 | Melanoma | DS |
| ME9384 | Melanoma | DS |
| SK12227 | Merkel cell | PD |
| SK12232 | Merkel cell | PD |
| LU5212 | NSCLC | DS |
| LU11554 | NSCLC | NE |
| LU11692 | NSCLC | DS |
| LU11951 | NSCLC | PD |
| LU5138 | NSCLC | DS |
| LU5165 | NSCLC | DS |
| LU5200 | NSCLC | DS |
| LU5355 | NSCLC | DS |
| OV15398 | Ovarian | DS |
| OV15631 | Ovarian | DS |
| OV5301 | Ovarian | DS |
| OV5304 | Ovarian | DS |
| LU5171 | SCLC | DS |
| LU5192 | SCLC | DS |
| LU5197 | SCLC | DS |
| LU5207 | SCLC | DS |
| LU5220 | SCLC | PD |
| LU5263 | SCLC | PD |

Mice engrafted with human PDX tumors were administered VACV-LUC at $10^7$ PFUs once weekly for 3 total doses and monitored for tumor growth inhibition relative to tumor volume at the time of treatment initiation. BOR was determined according to the following criteria: CR, no measurable tumor (100% response); PR, ≥30% decrease in tumor size from first dose at any time during or after 3-dose treatment; DS), tumor volume not meeting CR or PR criteria but showing <100% tumor volume increase either from first or third (final) dose sustained over a period of ≥14 days, with vehicle-treated tumor showing progressive tumor growth; PD, tumor volume growth not meeting CR, PR, or DS criteria and demonstrating progressive growth; nonevaluable (NE), not evaluable for BOR.

would amplify its immunostimulating properties. IL-12 is a well-characterized cytokine involved in the activation of both innate and adaptive immune systems and has shown promising results as an immunotherapy strategy.[22] Therefore, we generated a VACV encoding a recombinant human IL-12 fusion protein transgene (hereafter called AZD4820) in the viral TK locus under control of the late pF17R promoter with concomitant deletion of viral TK (Figure 2A). This IL-12 fusion protein consists of the p40 IL-12 subunit fused to the p35 IL-12 subunit by a flexible glycine-serine linker (G6S) to stabilize the IL-12 dimer. To further increase tumor-specific replication, the *I4L* gene encoding the viral RR was also deleted as previously described.[9] AZD4820 was generated and amplified in primary chicken embryo fibroblast (CEF) cells. AZD4820 replication kinetics and oncolytic activity in tumor cell lines were similar to those in control VACV (Figures S3A and S3B). IL-12 transgene secretion was detected in the supernatant of infected tumor cells, and bioactivity was confirmed with the HEK-Blue IL-12 SEAP reporter cell line, demonstrating that the bioactivity of viral IL-12 transgene was similar to that of recombinant human IL-12 (Figures 2B and 2C).

To characterize the oncolytic activity of AZD4820, *in vitro* cell killing was evaluated in 30 human cancer cell lines representing 12 tumor types. Tumor cells were infected over a range of MOIs with VACV-LUC or AZD4820, and cell killing was evaluated on day 5. Because the IL-12 receptor is primarily expressed on immune cells but not on tumor cells, we did not anticipate any difference in cell killing between VACV-LUC and AZD4820 in this *in vitro* setting in the absence of immune cells. VACV-LUC and AZD4820 effectively killed tumor cells at relatively low MOIs and demonstrated similar half-maximal oncolytic activity ($EC_{50}$) across tumor lines (Pearson $r = 0.94$; $p < 0.0001$), further indicating that encoding IL-12 did not interfere with VACV oncolysis (Figures 2D–2F). Cell lysis mediated by AZD4820 was broadly observed across tumor cell lines of different cancer types: 27 of 30 tumor cell lines showed mean $EC_{50}$s of MOI ≤0.1. Transgene expression and virus replication were also evaluated in the tumor cell lines 5 days after infection (0.004 MOI), showing broad evidence of replication and IL-12 production in cultured human cell

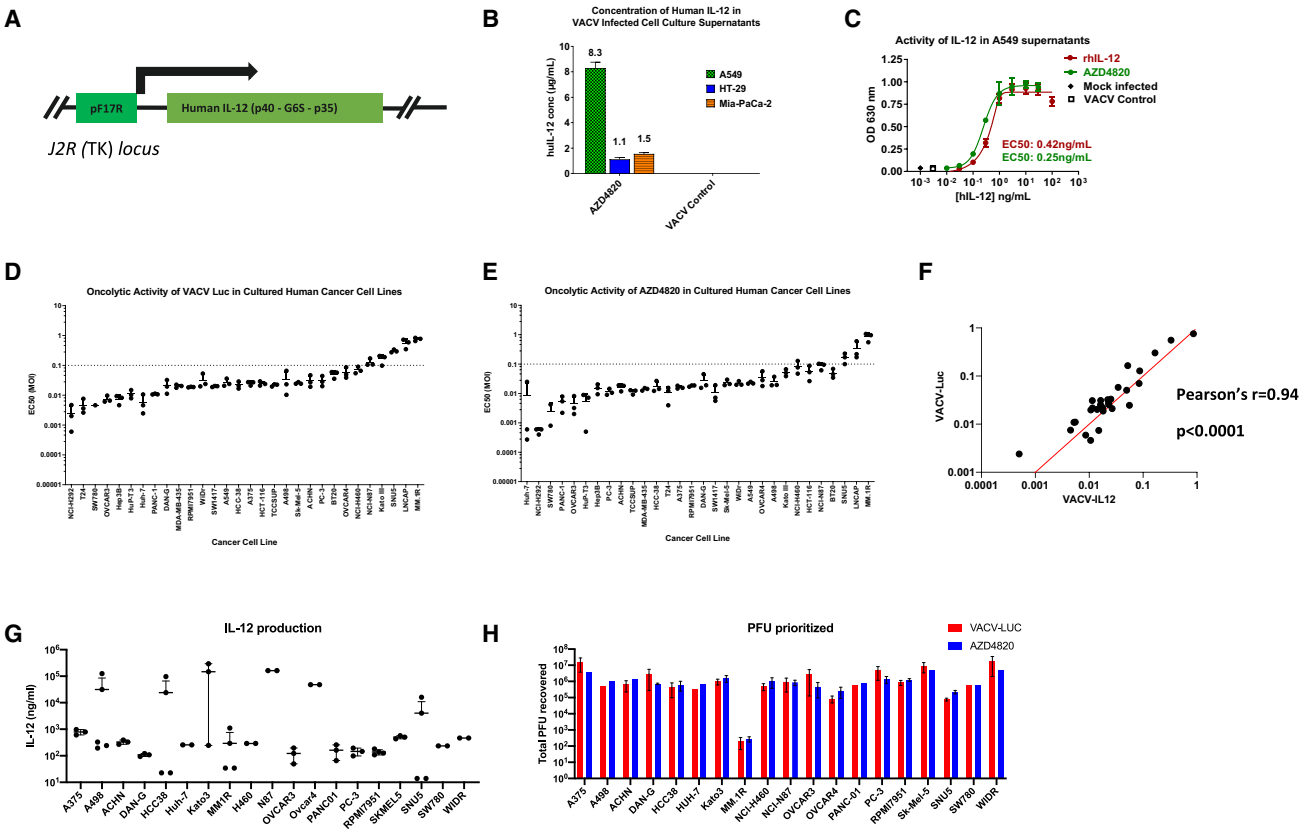


**Figure 2. IL-12 transgene expression and bioactivity, replication, and oncolytic activity of AZD4820 and VACV-LUC control virus in cultured human tumor cell lines**

(A) AZD4820 OV. pF17R, viral promoter driving expression of human IL-12 fusion protein consisting of p40 and p35 IL-12 subunits covalently linked by a G6S linker; promoter and transgene are inserted into the J2R viral locus, replacing the viral TK gene. (B) Expression of human IL-12 transgene in cell culture supernatants from human tumor cell lines infected by AZD4820 or empty VACV control virus at MOI of 0.01 for 72 h as measured by human IL-12–specific ELISA. Error bars represent standard deviation of the mean. (C) Bioactivity of IL-12 transgene measured by HEK Blue reporter cell assay in cell culture supernatants from AZD4820, empty VACV control, or mock-infected cells as compared with a titration of recombinant human IL-12 (rhIL-12). Error bars represent standard deviation of the mean. $EC_{50}$ values represent half-maximal IL-12 biological activity as determined by 4-parameter fit, nonlinear regression analysis of sigmoidal dose-response curves. (D and E) Oncolytic activity of VACV-LUC (D) and (E) AZD4820 across human tumor cell lines expressed as a mean MOI $EC_{50}$ oncolysis value (line) with each individual experimental $EC_{50}$ value represented as dots and SD of the mean as whiskers. Dotted line arbitrarily represents a mean MOI activity value of 0.1 for potency reference. (F) Statistical correlation between the mean MOI $EC_{50}$ oncolysis values between VACV-LUC and AZD4820 viruses across human tumor cell lines. (G) Human IL-12 transgene in cell culture supernatants of human tumor cells infected with AZD4820 at an MOI of 0.004 using 2,500 cells per well in 100 µL of medium at day 0 and supernatant collected at day 5 postinfection. Human IL-12 was measured by a human IL-12–specific electrochemiluminescence assay. Error bars represent standard deviation of the mean. (H) Recovery of virus from cells infected with AZD4820 or VACV-LUC control virus at MOI of 0.004 as measured by a virus plaque assay. Error bars represent standard deviation of the mean.

lines (Figures 2G and 2H). In addition, AZD4820 amplification was not observed in peripheral blood mononuclear cells (PBMCs) and minimal replication was seen in normal human hepatocytes and dermal fibroblasts, suggesting that replication is relatively selective for tumor cells (Table S2).

To determine the antitumor efficacy of AZD4820, immunodeficient NOD/SCID mice bearing subcutaneous human tumor cell line–derived xenografts (CDXs) (NCI-H292 lung, SW780 bladder, or HCT-116 CRC) were treated with a single intravenous dose of VACV-LUC or AZD4820 ($10$,[5] $10^6$, or $10^7$ PFUs, respectively) or vehicle (Figures 3A–3C). Significant tumor control was observed in the NCI-H292 and HCT-116 models following a single dose of $10^5$ PFUs of AZD4820 relative to vehicle-treated mice ($p < 0.001$). Significant tumor control was also observed in the SW780 model following a single dose of AZD4820 at $10^6$ PFU ($p < 0.001$). VACV-LUC and AZD4820 at the $10^7$ PFU dose both demonstrated tumor control in each model. This is attributable to the oncolytic activity of each virus and not to human IL-12 transgene produced by AZD4820, because NOD/SCID mice lack an intact immune system that is relevant for testing the biological activity of IL-12, and human IL-12 does not bind to the mouse IL-12 receptor.[30] These findings indicate that the oncolytic activity of VACV is a key contributor to tumor control in these preclinical models.

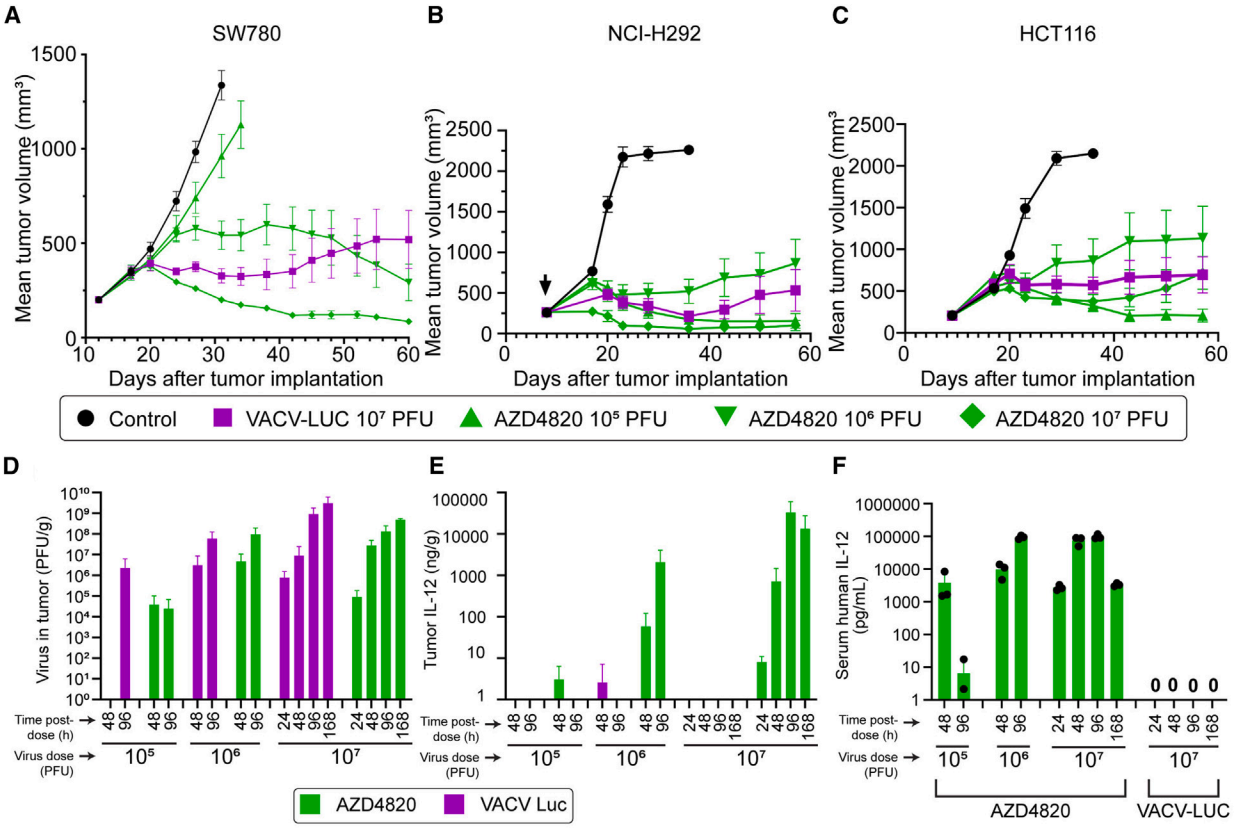


G

| Tissue | Treatment | Time post-dose | | | |
|---|---|---|---|---|---|
| | | 24 h | 48 h | 96 h | 168 h |
| Tumor | Vehicle | | | | |
| Tumor | 1e7 AZD4820 | | | | |
| Tumor | 1e6 AZD4820 | | | | |
| Tumor | 1e5 AZD4820 | | | | |
| Lung, liver, spleen, kidneys | 1e7 AZD4820 | | | | |
| Ovary | 1e7 AZD4820 | | | | |
| Ovary | 1e6 AZD4820 | | | | |
| Ovary | 1e5 AZD4820 | | | | |

% VACV IHC+ area: None; <5; 5–25; 26–50; 51–75; 76–100

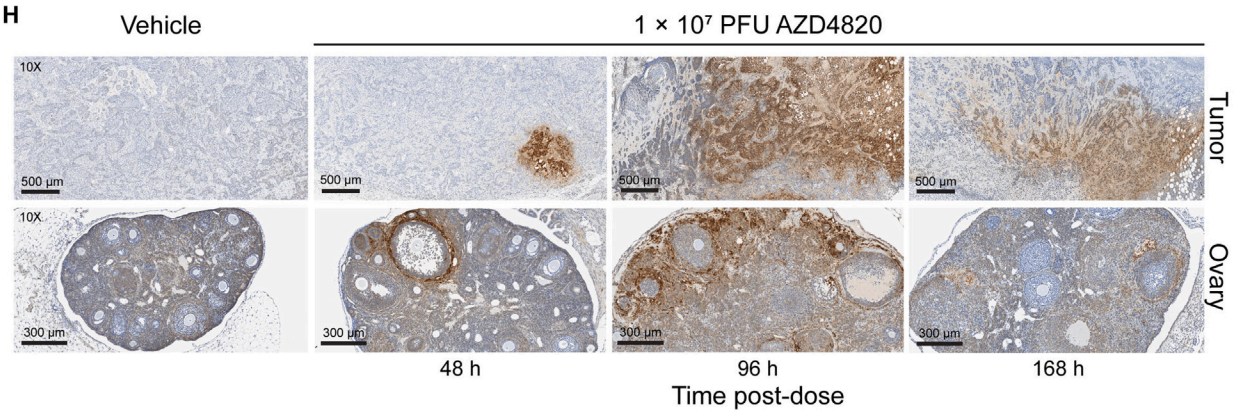


*(legend on next page)*

The kinetics of human IL-12 transgene production and replication was assessed in mice bearing SW780 bladder tumors. A dose- and time-dependent increase in virus replication was observed in the treated tumors. At 96 h after dosing, $2.5 \times 10^4 \pm 4.3 \times 10^4$ PFU/g (mean ± SD) was recovered from mice treated at $10^5$ PFUs, $9.5 \times 10^7 \pm 1.0 \times 10^8$ PFU/g was recovered from mice treated at $10^6$ PFUs, and $1.3 \times 10^8 \pm 1.2 \times 10^8$ PFU/g was recovered from mice treated at $10^7$ PFU (Figure 3D). Similarly, production of IL-12 increased over time in the tumor (Figure 3E). Human IL-12 was also detected in the peripheral blood, indicating the transfer of IL-12 from tissue to the circulation (Figure 3F).

Next, we evaluated virus replication within tumors of treated mice by immunohistochemistry (IHC). Mice bearing SW780 tumors were treated with vehicle or AZD4820 ($10,^5$ $10^6$, or $10^7$ PFUs), and tumor and normal tissues (lung, liver, spleen, kidneys, and ovaries) were collected at 24, 48, 96, and 168 h after dosing. VACV-specific IHC showed positivity in 5%–25% of cancer cells by 24 and 48 h after treatment with $10^7$ PFUs (Figures 3G and 3H). At this dose, the percentage of virus-positive cells peaked at 96 h after dosing, although the positive tumor area remained higher at 168 h than at 24 or 48 h. This pattern of virus IHC positivity reflects the replication and spread of virus within treated tumors. Virus-positive tumor cells were also observed in mice treated with $10^6$ PFU at 96 h but not at 48 h. Although virus could not be detected by IHC at the lowest dose ($10^5$ PFUs), live virus could be detected in tumors by plaque assay (Figure 3D). Mouse ovaries, but not other normal tissues, were also positive for VACV by IHC (Figures 3G and 3H).

### AZD4820 infection of tissue slice cultures (TSCs) and primary dissociated tumor cells

To evaluate AZD4820 infection in primary human tumor tissues, fresh TSCs were prepared from surgically resected melanoma, bladder, CRC, lung, renal, and ovarian cancers. These tumor TSCs, which maintain the structure and cell composition of the TME, were infected with AZD4820 (10 PFUs), a control VACV expressing GFP, or a mock infectious agent. IL-12 transgene production was then evaluated. Infection in the tumor TSC demonstrated that IL-12 was detectable in 22 of 22 (100%) slices (from 8 individual donors) treated with AZD4820 (12,440 ± 2,893 pg/mL), with low to undetectable levels in the VACV GFP-treated (2.05 ± 2.48 pg/mL) and mock-infected (1.96 ± 2.87 pg/mL) samples. The increased concentration of IL-12 in the AZD4820-treated cultures was highly significant (AZD4820 versus VACV GFP or mock infected; $p < 0.001$) (Figure 4A). Similar results were observed in primary dissociated tumor cell (DTC) cultures. AZD4820 infection resulted in the production of IL-12 in 19 of 19 (100%) DTC samples tested (17,984 ± 49,523 pg/mL). In contrast, minimal IL-12 concentrations were observed in the supernatants from the mock-infected and VACV GFP-treated cultures (6.15 ± 9.13 and 4.99 pg/mL, respectively; Figure S4A). IFN-γ induction is a key downstream cytokine induced upon IL-12 receptor signaling.[22] Although *IFNγ* gene expression after AZD4820 infection was significantly greater than after mock infection (1.5-fold; $p < 0.001$) or VACV GFP (1.4-fold; $p < 0.001$) in TSCs, evaluation of both TSC and DTC culture supernatants demonstrated that IFN-γ protein was not detected following AZD4820 treatment (Figures 4B, 4C, and S4B). VACV encodes several immunomodulatory genes that suppress immune cell activation, such as *B8R* and *B19R*, which sequester and neutralize IFN-γ and type I IFN, respectively.[5,14] As expected, AZD4820 infection of TSCs resulted in the expression of *B8R* (Figure 4D), which has been shown to sequester IFN-γ in the supernatant of infected cells[5] and probably accounts for the lack of detectable IFN-γ in the above experiments. Similarly, IFN-α2a and IFN-β were not induced in significant amounts upon VACV infection of DTCs (Figures S4C and S4D), consistent with the expression of *B18R*.

### Expression of IL-12 from VACV in an *in vivo* rat tumor model

Since IFN-γ signaling is critical for the efficacy of IL-12,[31] we sought to evaluate the impact of B8R on IL-12 and downstream IFN-γ activation in an *in vivo* system. VACV-encoded B8R does not bind murine IFN-γ; however, B8R binds and neutralizes IFN-γ from humans and rats.[5] To confirm the binding of B8R to rat IFN-γ, we performed a competitive ELISA. Recombinant B8R (rB8R) protein or filtered supernatant from VACV-infected HeLa cells were incubated with recombinant rat IFN-γ (1 ng/mL) for 1 h at 37°C. Next, an ELISA was performed to measure the available rat IFN-γ. Incubation with rB8R resulted in more than 50% neutralization, whereas supernatant from infected cells was able to inhibit the detection of IFN-γ in a dose-dependent manner, confirming that B8R binds rat IFN-γ (Figure 5A).

Based on the ability of B8R to bind rat IFN-γ, we used a syngeneic rat tumor model to evaluate AZD4820 in an immunocompetent model. We generated a surrogate virus encoding murine IL-12 (VACV muIL-12), since muIL-12 has been shown to cross-react with IL-12 receptors in rats[32] and is also an appropriate surrogate for studies in

**Figure 3. Antitumor efficacy and pharmacodynamics of AZD4820 in human CDX tumor models**

(A–C) Antitumor activity of vehicle (PBS + 0.05% BSA), VACV-LUC control virus, or AZD4820 administered once at the indicated intravenous doses in the (A) SW780 bladder, (B) NCI-H292 lung, and (C) HCT116 CRC xenograft models in immunodeficient mice. Error bars indicate SEM. *p = 0.033, ***p < 0001 for AZD4820-treated versus control-treated groups at day 31 for SW780, day 36 for NCI-H292, and day 36 for HCT-116, using 1-way ANOVA with Tukey correction for multiple comparisons. (D) AZD4820 or VACV-LUC virus recovered from SW780 bladder tumors at the indicated times after administration of a single intravenous dose of $10^5$, $10^6$, or $10^7$ PFUs of virus as indicated. Error bars represent standard deviation of the mean. (E) Detection of human IL-12 transgene in SW780 tumors from mice treated with a single $10^5$, $10^6$, or $10^7$ PFU intravenous dose of AZD4820 or VACV-LUC at the indicated time points after dosing. Error bars represent standard deviation of the mean (F) Detection of human IL-12 transgene in mouse plasma after a single intravenous dose of AZD4820 or VACV-LUC control virus. Error bars represent standard deviation of the mean. (G) Prevalence of $VACV^+$ cell area over time in SW780 tumors after single, intravenous administration of AZD4820 as indicated. Each box represents percent positive tumor cell area of the entire tumor as determined by VACV-specific IHC and read by a board-certified pathologist. (H) Representative staining of a tumor and normal ovary over time in an SW780 tumor-engrafted mouse treated with a single dose of $10^7$ PFUs of AZD4820. Bar represents 300 μm.

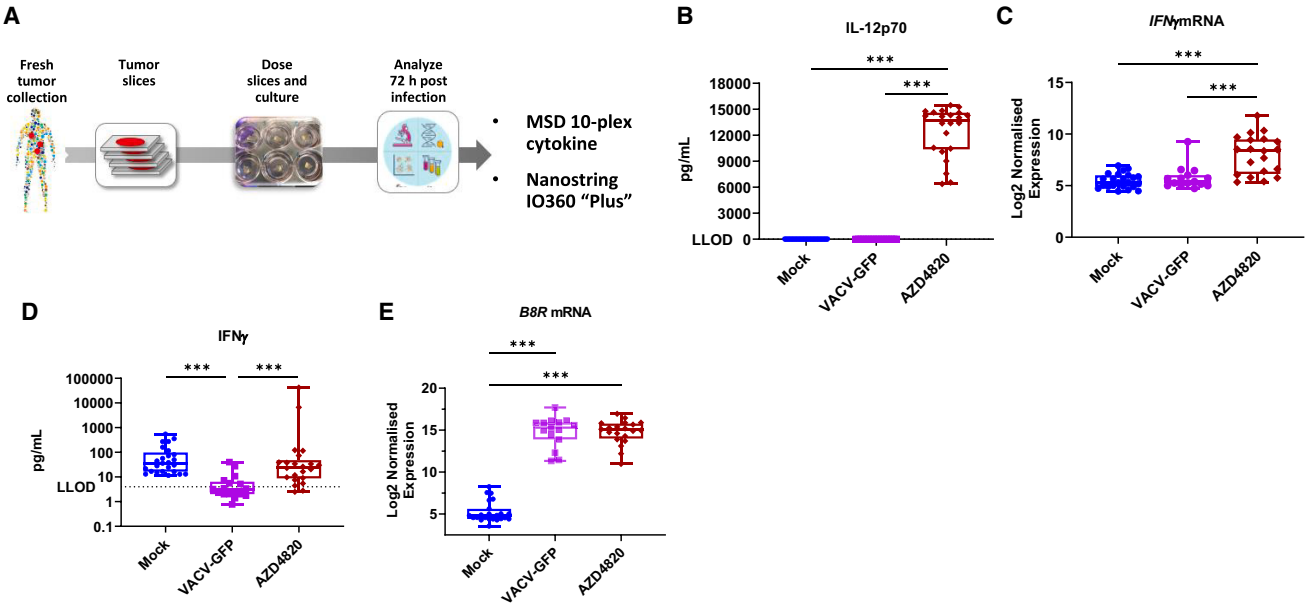


**Figure 4. AZD4820 infection and production of IL-12 in fresh primary human TSCs**

(A) Testing of AZD4820 infection, replication, and transgene production in cultured human tumor tissue slices treated with AZD4820 or VACV control virus or mock infected. (B) Detection of human IL-12 transgene in TSC supernatants from cultured tumor TSCs. Each dot represents an individual measurement of IL-12 cytokine from a TSC derived from melanoma, bladder, CRC, lung, renal, or ovarian cancer and represented by 25 (mock), 17 (VACV GFP), and 22 (AZD4820) slices derived from 8 individual donors. (C) IFN-γ transcript expression in TSCs. (D) IFN-γ protein detected in tumor TSC. (E) Viral B8R transcript expression in TSCs. Bar, median; boxes range from 25th to 75th percentile; whiskers extend to lowest and highest value. ***$p < 0.001$; ns, not significant (1-way ANOVA with Tukey post hoc comparison). LLOD, lower limit of detection.

mouse syngeneic tumor models. VACV muIL-12 demonstrated similar replication, oncolysis, and transgene bioactivity as AZD4820 in human and mouse tumor cells (Figure S5). VACV muIL-12 also effectively replicated in rat tumor cells, produced muIL-12 transgene, and effectively killed rat tumor cells (Figures 5B–5D). Rats were implanted with F98 tumor cells and treated with VACV-LUC ($10^7$ PFUs) or VACV muIL-12 (10,$^5$ $10^6$, or $10^7$ PFUs) on days 0, 4, and 7 by intravenous administration. Cytokine analysis of rat plasma confirmed the production of IL-12 p70 by VACV muIL-12, with a modest increase between rats treated with $10^5$ and $10^6$ PFUs. In addition, IFN-γ could be detected in the plasma of VACV muIL-12–treated rats, but not in the plasma of rats treated with VACV-LUC control. These results suggest that IL-12 encoded by VACV can induce peripheral IFN-γ production, which is not fully inhibited by viral B8R.

### Therapeutic efficacy of VACV expressing IL-12 in murine syngeneic tumor models

To further evaluate the immunomodulatory impact of IL-12, we tested the murine surrogate VACV muIL-12 virus in syngeneic murine tumor models. Mice bearing subcutaneous CT26 tumors were treated with five intratumoral doses ($10^7$ PFUs per dose) of the vehicle control, VACV-LUC, or VACV muIL-12 (Figure 6A). Treatment with VACV-LUC did not result in the control of CT26 tumors, and mean tumor volume was similar to that in the vehicle-treated group. However, treatment with VACV muIL-12 resulted in the regression of CT26 tumors, with 60% of engrafted mice surviving past day 39 (Figures 6B and 6C).

VACV-LUC and VACV muIL-12 demonstrated similar oncolytic activity and replication in murine tumor cells (Figure S6). Therefore, we hypothesized that the observed difference in tumor control could be attributed to the immunomodulating effects of muIL-12. Evidence of IL-12 cytokine accumulation in the plasma of mice was detected as early as 4 h after the injection of VACV muIL-12 (Figure 6D). Induction of IFN-γ is an important feature of IL-12 signaling and was detected in VACV muIL-12–treated mice at 4 and 24 h after injection (Figure 6E). Following the same treatment regimen, similar results were observed in the MC38 syngeneic tumor model. Treatment with VACV muIL-12 resulted in significant tumor growth control and prolonged survival, whereas VACV-LUC did not improve survival or tumor burden relative to vehicle-treated mice (Figures 6F and 6G). Moreover, IL-12 and IFN-γ induction was measured only in the plasma of VACV muIL-12–treated mice (Figures 6H and 6I). Overall, these results suggest that VACV encoding IL-12 engaged the innate and adaptive immune responses to control tumor growth, whereas the oncolytic activity of VACV-LUC alone was not sufficient to control the tumor burden in these models. The latter is an expected result given the poor oncolytic activity of VACV for murine tumor cells as compared with human tumor cells.

### Combination therapy of VACV muIL-12 with immune checkpoint inhibition

Although VACV muIL-12 resulted in significant tumor control (Figure 6), we hypothesized that immune activation elicited by VACV muIL-12 may upregulate PD-L1 in the TME and that combining

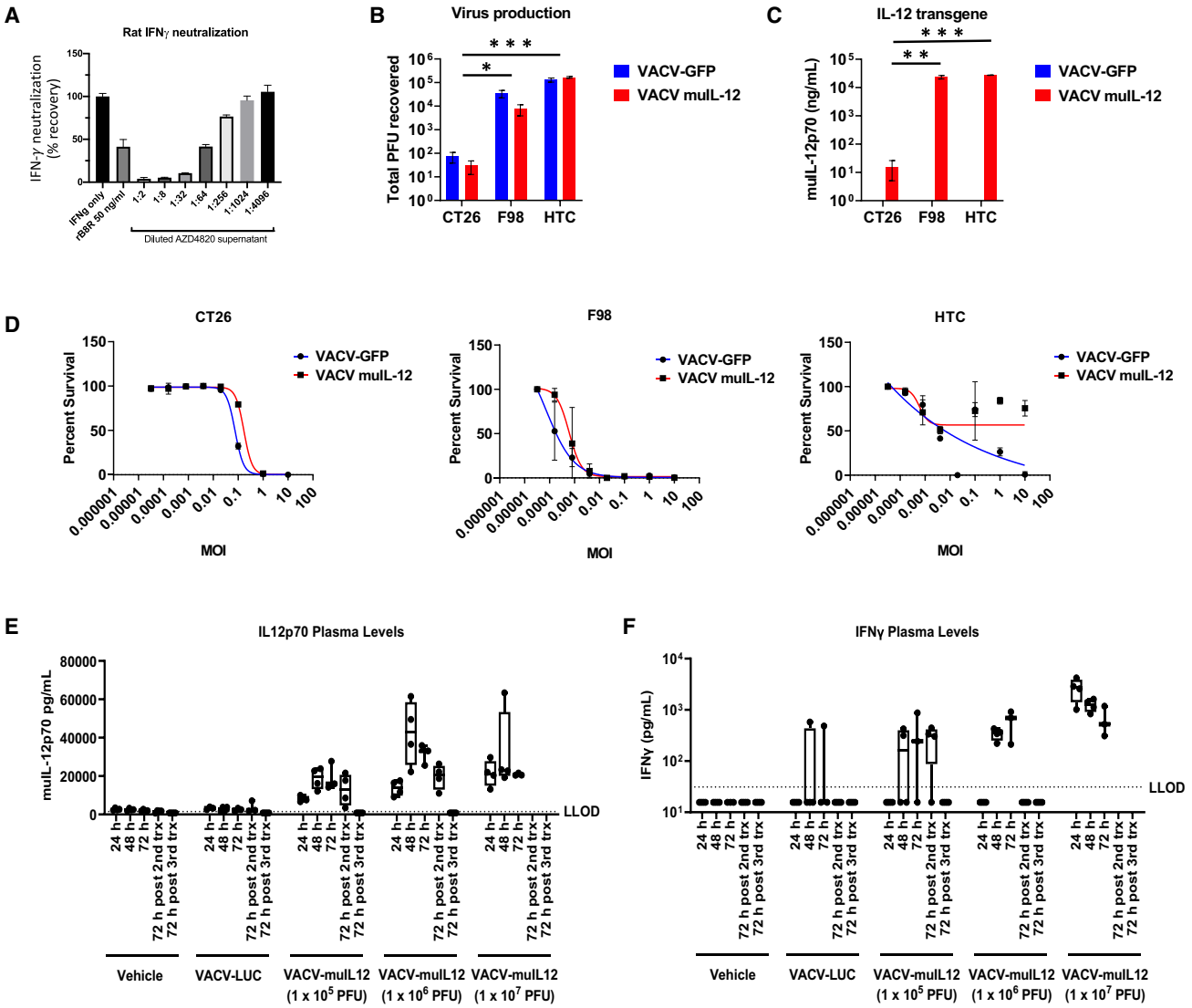


**Figure 5. VACV mulL-12 replication and production of mulL-12 in rat tumor cell lines**

(A) Neutralization of rat IFN-γ by cell culture supernatant removed from AZD4820-infected (MOI 1) HeLa cells and diluted with PBS as indicated or by 50 ng/mL recombinant B8R protein as positive control. (B) Replication of VACV mulL-12 or VACV GFP control virus in mouse CT26 CRC or rat F98 glioma and HTC HCC cultured cell lines measured by virus plaque assay. Error bars represent standard deviation of the mean. ***$p < 0.001$, *$p < 0.05$ unpaired, two-tailed Student's t-test. (C) Mouse IL-12 transgene production by mouse CT26 or rat F98 and HTC cultured cell lines treated with VACV mulL-12 or VACV GFP control virus as measured by mouse IL-12–specific electrochemiluminescence assay. Error bars represent standard deviation of the mean. ***$p < 0.001$, **$p < 0.01$ unpaired, two-tailed Student's t-test. (D) Oncolytic activity of VACV mulL-12 and VACV GFP control virus for mouse CT26 and rat F98 and HTC cell lines as measured by CellTiter-Glo luminescent cell viability assay (Promega). Error bars represent standard deviation of the mean. (E) Plasma levels of mouse IL-12 transgene in rats engrafted with subcutaneous rat F98 glioma tumors and administered intravenous VACV mulL-12 at $10^5$, $10^6$, or $10^7$ PFUs; VACV-LUC control virus at $10^7$ PFU; or vehicle (PBS + 0.05% BSA). (F) Plasma levels of rat IFN-γ in treated rats. Bar, median; boxes range from 25th to 75th percentile; whiskers extend to lowest and highest values.

the VACV muIL-12 surrogate with immune checkpoint inhibition could enhance antitumor T cell immunity. To test this hypothesis, mice were engrafted with CT26 tumors and treated with vehicle, VACV-LUC, or VACV muIL-12, either as monotherapies or in combination with isotype control, or with an anti-mouse PD-L1 blocking antibody (Figures 7A–7D). Interestingly, we did not observe a significant enhancement in tumor control when VACV muIL-12 was delivered in combination with anti-PD-L1 antibodies, perhaps because CT26 tumors were well controlled following VACV muIL-12 therapy alone. However, upregulation of PD-L1 on immune cells in VACV muIL-12–treated tumors was observed (Figures 7E–7G and S7), indicating immune activation of antigen-presenting cells by virus and/or

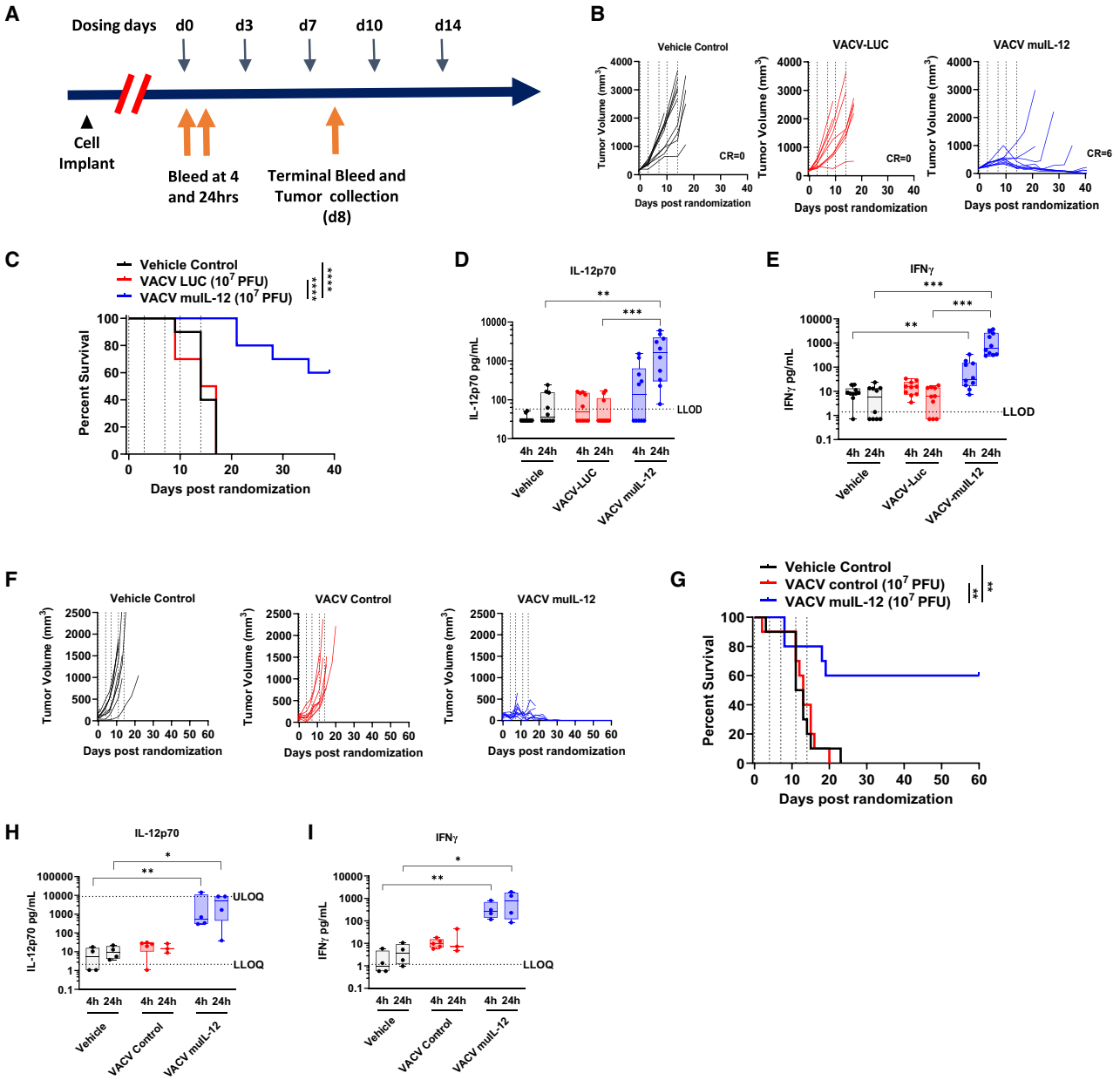


**Figure 6. VACV mulL-12 enhancement of antitumor immune response in murine syngeneic CT26 and MC38 tumor models**

(A) Study schema for the use of VACV mulL-12 in the CT26 and MC38 CRC models. After cell implantation, tumor growth was monitored and mice were randomized to study groups based on tumor volume. Thereafter, mice were treated with intratumoral vehicle (PBS + 0.05% BSA), VACV-LUC control, or VACV mulL-12 viruses twice weekly for 5 doses as indicated. Peripheral blood was collected at 4 and 24 h for preparation of plasma to measure peripheral blood cytokine levels, and mice were terminally sacrificed at day 8 to examine intratumoral pharmacodynamic endpoints. (B) Tumor growth curves showing the antitumor activity of VACV mulL-12 relative to that of vehicle or VACV-LUC control virus–treated mice engrafted with CT26. The proportions of tumors showing CR to treatment are indicated above the graphs. Dotted lines indicate the timing of test article treatment. (C) Kaplan-Meier survival curve analysis of CT26 tumor-engrafted mice. ****$p < 0.0001$, log rank test. (D) Murine IL-12 detection in plasma of CT26 tumor-engrafted mice at 4 or 24 h after test article administration. (E) IFN-γ in plasma from CT26 tumor-engrafted mice. Dots = individual mice; box hinges = 25th and 75th percentiles; box midline = median; whiskers = minimum to maximum distribution. Statistical analysis was performed on log transformed data and analyzed by Kruskal-Wallis test and Dunn multiple comparisons test. **$p < 0.01$; ***$p < 0.001$; ****$p < 0.0001$. (F) Tumor growth curves showing the antitumor activity of VACV mulL-12 relative to that of vehicle or VACV-LUC control virus–treated mice engrafted with MC38. (G) Kaplan-Meier survival curve analysis of MC38 tumor engrafted mice. **$p < 0.01$, log rank test. Dotted lines indicate the timing of test article treatment. (H) Murine IL-12 in mouse plasma at 4 or 24 h after test article administration to MC38 tumor-engrafted mice. (I) IFN-γ in plasma from MC38 tumor-engrafted mice. Bar, median; boxes range from 25th to 75th percentile; whiskers extend to lowest and highest values.

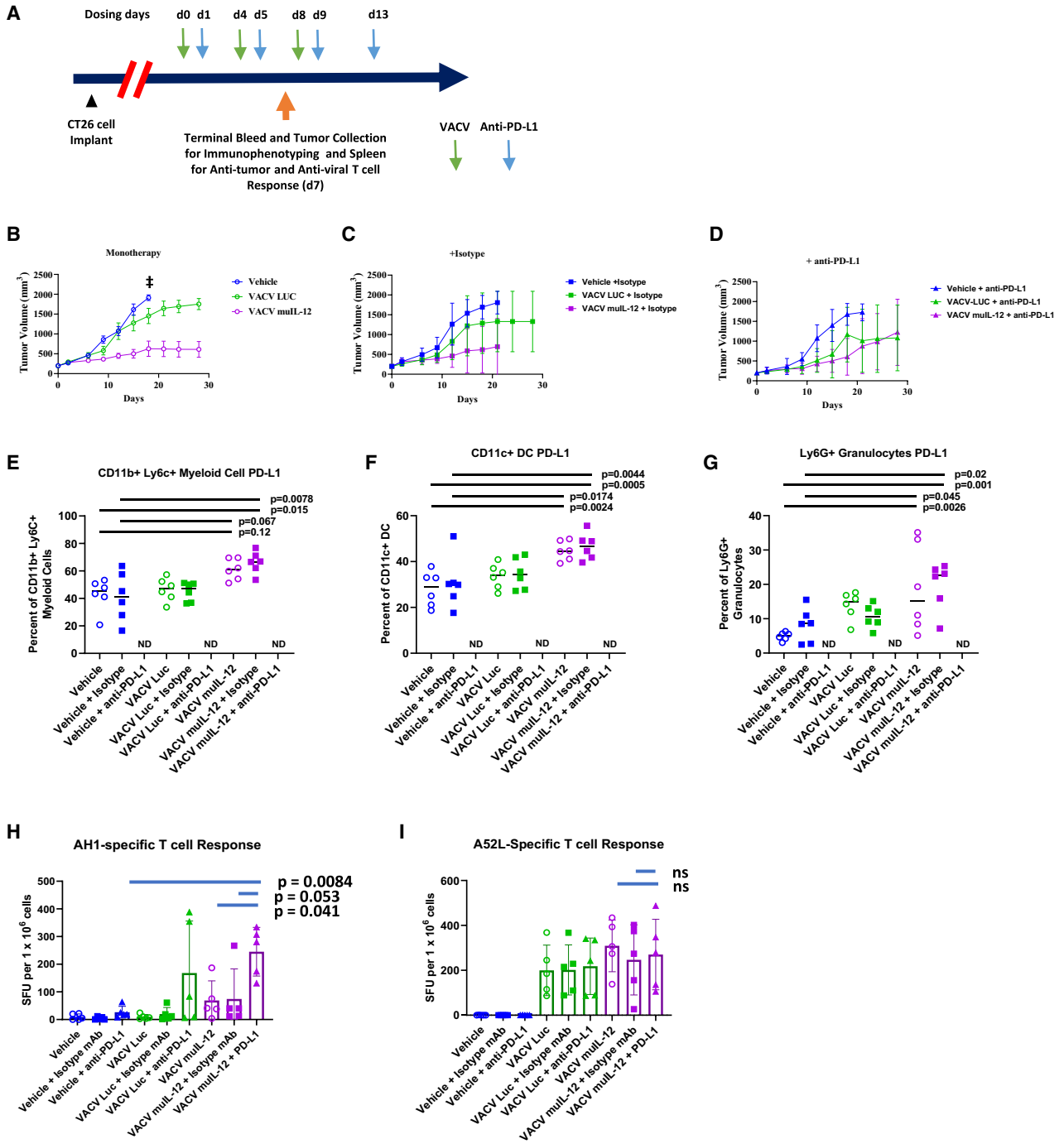


**Figure 7. Effect of VACV mulL-12 combined with anti–PD-L1 on antitumor T cell immunity in the CT26 model**

(A) Study schema for VACV mulL-12 administered in combination with anti-mouse PD-L1 mAb in the CT26 CRC model. Tumors were collected on day 7 and dissociated for immunophenotyping. (B) Tumor growth curves for CT26 tumors treated with vehicle, VACV-LUC, or VACV mulL-12 as monotherapies. ‡$p < 0.0001$ for mean tumor volume differences between vehicle versus VACV mulL-12 and $p = 0.0035$ for VACV-LUC versus VACV mulL-12–treated groups at day 18 using 1-way ANOVA with Tukey correction for multiple comparisons. (C) Tumor growth curves for mice treated with vehicle, VACV-LUC, or VACV mulL-12 combined with isotype control antibody. Error bars represent the standard deviation of the mean. (D) Tumor growth curves of mice treated with vehicle, VACV-LUC, or VACV mulL-12 combined with anti-mouse PD-L1 antibody. (E) Cell surface PD-L1 expression on $CD11b^+$ $Ly6C^+$ myeloid cells in the TME of CT26 tumors treated with the indicated test articles. (F) Cell surface PD-L1 expression on $CD11c^+$

*(legend continued on next page)*

muIL-12 transgene activity. Likewise, increased cell surface PD-L1 was seen on the $CD45^-$ cell population comprising tumor cells plus nonimmune stroma (e.g., fibroblasts, endothelial cells, pericytes) within the tumor microenvironment (Figure S7).

As a result of immune activation in the TME, it is reasonable to hypothesize that changes in the frequency or activation status of T cells may be observed. Interestingly, we did not see changes in the frequency of CD45 immune cells or in the frequency or activation (defined by CD69 cell surface levels) of conventional CD4 ($FoxP3^-$), CD8, or regulatory CD4 T cells ($FoxP3^+$) in the tumor at 3 or 7 days postfirst dose of virus (Figure S8). It is conceivable that these time points did not capture changes in T cell dynamics within the tumor. Alternatively, it is possible that a smaller proportion of tumor-specific T cells primed by activated antigen-presenting cells were affected by the muIL-12 transgene.

To assess a tumor-specific T cell response after therapy, splenocytes were collected on day 7 after VACV dosing and stimulated with either a tumor-associated peptide antigen (AH-1) or a VACV-specific peptide (A52L). Combining VACV muIL-12 with anti-PD-L1 resulted in a significant increase in the number of IFN-γ-secreting cells upon AH-1 peptide stimulation (VACV muIL-12 versus VACV muIL-12 plus anti-mouse PD-L1, $p = 0.041$; anti-mouse PD-L1 versus VACV muIL-12 plus anti-mouse PD-L1, $p = 0.0084$) (Figure 7H). In comparison, VACV-LUC alone or in combination with anti-mouse PD-L1 did not result in a significant increase in IFN-γ-secreting cells relative to the other treatment groups. In addition, the VACV-specific (A52L) immune response was not affected by IL-12 expression by VACV muIL-12 or anti-mouse PD-L1 at the time point assessed (Figure 7I). Overall, these results suggest that VACV muIL-12 in combination with anti-PD-L1 blocking antibodies elicited an antitumor T cell immune response.

## DISCUSSION

OVs have been engineered to replicate and lyse tumor cells after intratumor, local, or intravenous (systemic) administration while selectively sparing normal cells. Vaccinia viruses have been developed as oncolytic agents due to their immune evasion, strong lytic potential, ability to avoid complement- and neutralizing antibody–mediated clearance, large coding capacity for transgenes, and potential to induce immunogenic cell death.[33] This latter feature of VACVs is demonstrated by the finding that oncolytic vaccinia viruses activate both innate and adaptive immune responses after injection into tumors in immunocompetent hosts.[34–36] Immune activation following virus replication and cell lysis can lead to enhanced tumor antigen cross-presentation by professional antigen-presenting cells, priming of antitumor T cell immunity, and production of tumor-specific antibodies by activated B cells, all of which contribute to an *in situ* vaccination against tumor.[18,19,33,37] Upregulation of immunosuppressive factors such as immune inhibitory cytokines and metabolites, as well as the PD-L1 and CTLA-4 checkpoint proteins in the TME, may serve to limit virus-induced antitumor immune responses.[27,34,35,38,39]

To build on the *in situ* vaccination potential of VACV and to counterbalance immunosuppression, VACV OVs have been engineered to express immune-stimulatory transgenes, including cytokines such as GM-CSF, IL-2, IL-23, IL-12, and IL-7; T cell–engaging bispecific antibodies; and immune checkpoint inhibitory antibodies targeting PD-1, PD-L1, or CTLA-4.[8,27,35,36,40] Many of these immunomodulatory proteins are potent immunostimulators that can cause significant immune-related toxicities when administered systemically as free drugs at biologically active doses. By delivery through a viral transgene, the expression of these immunostimulatory molecules may be concentrated in the TME to limit systemic exposure and immune-related toxicity. Although these transgenes hold the promise of inducing additive or synergistic antitumor activity when combined with the oncolytic potential of VACV, they could induce antiviral immunity to limit the replication and oncolysis of the virus. This may have an impact on virus spreading, transgene expressing, and tumor cell killing. Therefore, the impact of a viral transgene on antitumor and viral immunity and the effects of combination immunotherapy approaches must be determined empirically for each engineered virus.

Here, we report for the first time the design, generation, and characterization of AZD4820, a novel oncolytic vaccinia virus expressing a human IL-12 cytokine transgene. In our studies, the VACV platform (VACV-LUC) demonstrated antitumor activity across a range of PDX tumor types, including bladder, CRC, HCC, HNSCC, melanoma, NSCLC, ovarian cancer, and small cell lung cancer. Antitumor activity (CR + PR) was strongest in HNSCC, NSCLC, and melanoma and was not observed in Merkel cell PDX xenografts ($n = 2$). Oncolysis was the sole mechanism of action for the tumor control observed in the PDX studies because tumor-engrafted mice lacked an intact immune system. In clinical trials, the good response of tumor types to the biological effects of the IL-12 may translate into additional clinical benefit in patients treated with AZD4820. AZD4820 itself demonstrated *in vivo* antitumor activity against bladder, CRC, and NSCLC CDX tumors in immunodeficient mice and potent *in vitro* oncolytic activity against tumor cell lines originating from 12 different solid tumor types. Minimal-to-moderate *in vitro* activity was seen in a multiple myeloma cell line and a handful of solid tumor cell lines. Overall, however, results showed that VACV is a potent oncolytic agent capable of antitumor activity

DCs. (G) Cell surface expression of PD-L1 on $Ly6G^+$ granulocytes. Values represent the percentage of gated cells that were positive by flow cytometry for PD-L1 compared with staining controls. (H) AH-1-specific T cell response measured by IFN-γ ELISpot using splenocytes isolated from mice treated with test articles as indicated. (I) A52L virus peptide stimulated responses in splenocytes from treated mice. Statistical differences (p values) between treatment groups were determined using 1-way ANOVA with Tukey correction for multiple comparisons. Error bars represent the standard deviation of the mean. ND, not determined due to competition between fluorochrome-labeled anti-PD-L1 flow cytometry antibody and anti-PD-L1 blocking antibody treatment.

across numerous tumor types at doses anticipated to be clinically achievable following intravenous administration. Furthermore, AZD4820 was relatively selective for tumor-cell oncolysis *in vitro* when compared with cultured normal human cells, including PBMCs, dermal fibroblasts, and hepatocytes. These findings suggest that AZD4820 has been successfully engineered to minimize the spread of virus among normal tissues, although it is not completely devoid of such activity; the virus was detected in mouse ovaries and skin after the administration of AZD4820 to SW780 bladder tumor–engrafted mice.

AZD4820 is engineered to express a human IL-12 transgene consisting of the IL-12 p40 and p35 subunits covalently linked by a flexible glycine-serine linker (G6S) to enhance cytokine stability. The IL-12 transgene was chosen to amplify the immunogenic cell death and *in situ* vaccination properties of VACV through the enhancement of innate and adaptive immunity. Human IL-12 transgene expression was observed across AZD4820-infected human tumor cell lines *in vitro* and had biological activity equivalent to that of recombinant, disulfide-linked human IL-12 p40/p35 heterodimers. Moreover, the IL-12 transgene was detected in both the tumor lysates and peripheral blood of immunodeficient mice engrafted with human SW780 bladder tumors. This indicates that IL-12 produced by AZD4820-infected tumor cells *in vivo* entered the bloodstream, making this a potential pharmacodynamic marker of AZD4820 infection and replication in cancer patients. AZD4820 infection led to the production of IL-12 in primary human tumor tissue slice cultures and dissociated tumor cells, whereas VACV-LUC control virus did not. This demonstrates that IL-12 can be successfully produced by tumor tissue excised directly from cancer patients. However, IFN-γ was not detectable in these closed culture systems, despite an induction of IFN-γ mRNA that is anticipated downstream of IL-12 receptor signaling. Lack of IFN-γ protein detection was not unexpected because the viral B8R protein is known to bind and sequester human IFN-γ, and RNA encoding viral B8R protein was detected in the cultures.

Because IFN-γ is a critical effector of IL-12–mediated antitumor immunity,[30] it was important to assess whether viral B8R would bind and effectively inhibit IFN-γ in an *in vivo* system. To this end, we turned to a rat syngeneic tumor model, because rat IFN-γ binds to and is neutralized by VACV viral B8R protein.[5] Treatment of fully immunocompetent rats engrafted with the syngeneic glioma tumor cell line F98 resulted in the detection of IL-12 transgene in the peripheral blood. Likewise, elevated rat IFN-γ was also detected in peripheral blood, demonstrating that the production of IL-12 transgene by infected tumor cells induced enough IFN-γ over time to overcome neutralization by viral B8R.

To further explore the role of IL-12 in the antitumor activity of AZD4820, we administered a murine surrogate virus expressing mouse IL-12 (VACV muIL-12) to fully immunocompetent mice engrafted with syngeneic mouse tumors. Mouse IL-12 expressed by infected tumor cells was biologically active, but the virus itself showed relatively poor replication in mouse tumor cell lines, necessitating administration of the virus by the intratumoral route to mimic the amount of AZD4820 in engrafted human tumor xenografts when administered by the intravenous route. In this setting, VACV muIL-12 demonstrated antitumor activity and enhanced survival of mice engrafted with either CT26 or MC38 tumors where VACV control virus was not active. Mouse IL-12 protein was detectable in the peripheral blood of treated mice, indicating the production and movement of IL-12 from tumor to peripheral blood. Mouse IFN-γ was also induced in response to IL-12 production, because this cytokine was significantly elevated in the peripheral blood of mice treated with VACV muIL-12 but not mice treated with VACV control virus. These results, together with the antitumor activity of AZD4820 seen in PDX and CDX models in immunodeficient mice, suggest that both the immunomodulating and oncolytic properties of an IL-12–expressing VACV may be important for tumor control. In this context, it is encouraging that VACV muIL-12 in combination with anti-mouse PD-L1 blockade resulted in enhanced tumor-specific (AH-1) T cell immunity compared with the respective monotherapies. However, additive antitumor activity was not seen in these experiments. This may reflect the relatively strong activity of VACV muIL-12 monotherapy at the dose level used, the schedule of virus and immune checkpoint therapy, or underlying biology. This is an active area of investigation.

Results of preclinical research involving IL-12 expressing VACVs generated by other investigators support the potential utility of an oncolytic virus expressing this transgene as an anticancer therapy. For example, Nakao et al. showed that a VACV of the LC16mO strain (vaccinia virus growth factor and O1L deleted with B5R modified to reduce immunogenicity) engineered to express murine IL-12 resulted in numerical increases in intratumoral CD8 and CD4 T cells, major histocompatibility complex class $II^+$ macrophages, NKT cells, and NK cells relative to control virus and elicited antitumor activity when administered as a monotherapy by the intratumoral route in the LLC mouse syngeneic lung tumor model.[35] When virus was engineered to express IL-7 cytokine in addition to muIL-12, enhanced tumor-infiltrating T and NK cell percentages were observed and correlated with enhanced antitumor efficacy, abscopal antitumor effects on noninjected tumors, and superior antitumor activity when combined with anti-PD-1 or anti-CTLA-4 immune checkpoint therapy. It remains to be seen whether the addition of other immunomodulating cytokines along with IL-12 represents an oncolytic viral therapy that can be delivered safely in the clinic to enhance antitumor activity.

Another study by Ge et al. characterized the preclinical activity of a VACV Western Reserve strain (vaccinia virus growth factor and TK double deleted) engineered with either secreted or membrane-bound forms of a mouse IL-12 transgene.[41] This work demonstrated that either soluble or membrane-bound forms of murine IL-12 expressed by VACV delivered intraperitoneally can mediate potent antitumor immunity, resulting in the control of tumor growth and the enhanced survival of mice engrafted with syngeneic CRC or peritoneal mesothelioma tumors. The authors found that a membrane-bound form of IL-12 resulted in less kidney and lung edema

and lower serum levels of liver enzymes indicative of liver damage in mice when compared with VACV expressing the soluble IL-12 form. This observation suggests that the tethering of IL-12 to the plasma membrane may help reduce unwanted toxicity by free IL-12 transgene released into the peripheral blood. Further research is needed to determine whether this strategy to enhance the safety of VACV-mediated IL-12 delivery results in increased tolerability in patients with cancer.

Based on previously published studies of IL-12 delivery by VACV[35,41] and the preclinical evaluation of AZD4820 presented herein, we believe that this OV represents a promising oncolytic and immunotherapeutic agent for the treatment of cancer. The IL-12 produced by infected tumor cells was detected in peripheral blood and represents a potentially important translational endpoint to monitor in human clinical trials. Likewise, the correlation of virus replication and IL-12 production within tumor tissue with clinical response should be assessed. We did not directly measure virus-neutralizing monoclonal antibody (mAb) levels in preclinical treatment models in which multidose regimens were used. It is possible that neutralizing antibodies may be produced in patients treated repeatedly with intravenous AZD4820. This can be measured in human clinical trials and compared with virus levels in peripheral blood as well as virus replication and IL-12 transgene levels in tumor tissue following multiple doses. It is encouraging that other clinical trials using the oncolytic vaccinia virus Pexa-Vec administered intravenously or intratumorally showed pharmacodynamic and antitumor activity despite preexisting (baseline) or VACV-induced antivirus neutralizing antibody responses.[4,8,42] Finally, when considering AZD4820 as an immunotherapeutic agent, it will also be important to understand the relationship between changes in innate and adaptive immunity and AZD4820-mediated pharmacodynamic and clinical responses.

## MATERIALS AND METHODS

### Study design

The objective of this study was to generate a vaccinia virus expressing IL-12 (AZD4820) to enhance antitumor activity by engaging innate and adaptive immunity. The oncolytic activity of AZD4820 was evaluated *in vitro* using cell lines, primary TSCs, and primary DTCs. AZD4820 activity was demonstrated in human CDXs and syngeneic rodent tumors engrafted in immunocompetent rats and mice. In addition, AZD4820 was tested in combination with an anti-mouse PD-L1 checkpoint inhibitor. Antitumor immune responses were characterized by *ex vivo* splenocyte restimulation assays.

### Cell culture

Cell lines were obtained from the AstraZeneca cell bank and cultured as described in Table S3. Cells were authenticated through species-specific cell line authentication performed by IDEXX Bioanalytics (Westbrook, ME), using short tandem repeat DNA profiling and multiplex PCR-based testing. Cells were routinely tested for *Mycoplasma* contamination by a PCR-based method using the MycoSEQ Mycoplasma detection kit (catalog no. 4460623, Thermo Fisher Scientific, Waltham, MA). Cells used *in vivo* in antitumor efficacy and pharmacodynamic studies were tested for rodent viral pathogens with the IMPACT II mouse PCR-based pathogen testing from IDEXX Bioanalytics. Primary normal human hepatocytes were obtained from Lonza (Rockville, MD) and cultured according to the manufacturer's protocol. Fresh PBMCs were obtained from Lonza and AstraZeneca's internal blood donor program. All of the cells were cultured at 37°C with 5% $CO_2$.

### Vaccinia viruses

All of the recombinant vaccinia viruses used in this study were derived from the Copenhagen strain deleted in the *J2R* (TK) and *I4L* (RR) genes. COPTG19104 is a VACV expressing the fluorescent protein mCherry under the control of the pH5R promoter at the *J2R* locus and deleted in the *I4L* gene. This was used as the parental virus to generate AZD4820 and VACV muIL-12 (described below). VVTG18058 is a vaccinia virus deleted in the *J2R* and *I4L* genes and was used as the unarmed control virus in the MC38 syngeneic tumor model and *in vitro* as indicated. VACV-LUC is a VACV expressing firefly luciferase under the control of the p11k7.5 promoter in the *TK* locus and deleted in the *I4L* gene. VACV-GFP is a VACV expressing enhanced GFP under the control of the p11K7.5 promoter in the *TK* locus and deleted in the *I4L* gene.

### Generation of AZD4820 and murine surrogate

Recombinant VACV expressing human IL-12 (AZD4820) or murine IL-12 (VACV muIL-12) were generated from an attenuated Copenhagen strain VACV described previously.[43] Briefly, the recombinant viruses were generated by homologous recombination in CEFs, using COPTG19104 as starting parental virus and the transfer plasmids pTG19673 encoding human IL-12 or pTG19846 encoding murine IL-12 under the control of pF17R. COPTG19104 contains the expression cassette of the mCherry protein in its *J2R* locus. The homologous recombination between the transfer plasmid and parental vaccinia virus enabled the generation of recombinant vaccinia viruses that have lost the mCherry expression cassette and gained the human IL-12 (AZD4820) or the murine IL-12 (VACV muIL-12) expression cassettes. AZD4820 and VACV muIL-12 were sequence verified, propagated in CEFs, and titrated on Vero cells as previously described.[43]

### Plasmids and sequences

The VACV transfer plasmid pTG19535 was designed to allow insertion of the nucleotide sequence to be transferred by homologous recombination into the *J2R* locus of the VACV genome. It originates from the plasmid pUC18 into which was cloned the flanking sequences (BRG and BRD) surrounding the *J2R* locus. The plasmid pTG19535 contains the pF17R promoter.

The primary protein structure of the huIL-12 transgene consists of a fusion of the IL-12 p40 subunit (bold and with signal sequence underlined below) with the IL-12 p35 subunit (in italics; signal sequence absent) linked by a seven-amino acid polypeptide linker (bold and underlined):

MCHQQLVISWFSLVFLASPLVA**IWELKKDVYVVELDWYPDAP GEMVVLTCDTPEEDGITWTLDQSSEVLGSGKTLTIQVKEFGD AGQYTCHKGGEVLSHSLLLLHKKEDGIWSTDILKDQKEPKN KTFLRCEAKNYSGRFTCWWLTTISTDLTFSVKSSRGSSDPQG VTCGAATLSAERVRGDNKEYEYSVECQEDSACPAAEESLPIEV MVDAVHKLKYENYTSSFFIRDIIKPDPPKNLQLKPLKNSRQV EVSWEYPDTWSTPHSYFSLTFCVQVQGKSKREKKDRVFTDK TSATVICRKNASISVRAQDRYYSSSWSEWASVPCS**GGGGGGS *RNLPVATPDPGMFPCLHHSQNLLRAVSNMLQKARQTLEFYPCT SEEIDHEDITKDKTSTVEACLPLELTKNESCLNSRETSFITNGSCLA SRKTSFMMALCLSSIYEDLKMYQVEFKTMNAKLLMDPKRQIFLD QNMLAVIDELMQALNFNSETVPQKSSLEEPDFYKTKIKLCILLHA FRIRAVTIDRVMSYLNAS*.

The late poxvirus promoter pF17R was used: AAAATATAGTA GAATTTCATTTTGTTTTTTTCTATGCTATAA.

#### Cell killing, virus production, and transgene production

To assess cell killing, human tumor and normal cells were plated in 96-well, flat-bottomed plates (2,500 cells/well). Cells were infected with VACV-LUC, AZD4820, or VACV muIL-12 at MOIs of 10, 1, 0.1, 0.02, 0.004, 0.0008, 0.00016, and 0.000032 in a volume of 100 μL. Cell killing was determined on day 5 after infection using CellTiter Blue cell viability assay (Promega, Madison, WI) according to the manufacturer's protocol.

To assess VACV replication in human tumor and normal cells (*in vitro)*, cells were plated in 96-well, flat-bottomed plates (2,500 cells/well). Cells were infected with VACV-LUC, AZD4820, or VACV muIL-12 (0.004 MOI) in a volume of 100 μL. Infection supernatant was removed; cells were detached from cell culture plastic using trypsin solution, suspended in cell culture medium, and pelleted by centrifugation; and cell pellets were freeze-thawed twice. Quantification of virus was measured by plaque assay as described below.

Transgene production (huIL-12 or muIL-12) was measured in the supernatant on day 5 from tumor cells infected at an MOI of 0.004. VACV-LUC was used as a control. Human IL-12 and murine IL-12 concentrations were measured using the U-Plex human IL-12p70 assay and the U-PLEX mouse IL-12p70 assay (catalog nos. K151UAK and K152UAK; Meso Scale Diagnostics, Rockville, MD), respectively, according to the manufacturer's protocol.

To evaluate cell killing, transgene production, and virus replication in rat tumor cells, the same protocol was followed as described above but seeded at 10,000 cells/well. Normal human hepatocytes were plated at 50,000 cells/well for VACV infection assays.

#### IL-12 bioactivity assay

HEK-Blue IL-12-SEAP reporter cells (InvivoGen, San Diego, CA) were used to detect the bioactivity of VACV-produced human or murine IL-12. A total of 50,000 HEK-Blue IL-12 reporter cells were plated in 96-well, round-bottomed plates in 180 μL of culture medium. Supernatant from SW780 cells infected with VACV-LUC, VACV muIL-12, or AZD4820 (0.004 MOI) was filtered through a 0.1-μm filter to remove VACV particles. IL-12 concentration in the filtered supernatant was measured using an IL-12–specific electrochemiluminescence assay (MSD-ECL; Meso Scale Diagnostics), as described above. Culture medium (negative control), recombinant human IL-12 consisting of disulfide-linked p35 and p40 subunits (catalog no. 200-12; Peprotech, Rocky Hill, NJ), or the diluted infection supernatants were added to the HEK-Blue IL-12 reporter cells and incubated overnight at 37°C. Secreted embryonic alkaline phosphatase (SEAP) reporter activity was measured using QUANTI-Blue solution (InvivoGen) according to the manufacturer's protocol.

#### Tissue slice cultures and dissociated tumor cells

Fresh human tumor samples obtained from surgical resections of melanoma, bladder, CRC, lung, renal, and ovarian cancers were obtained from BioIVT (Westbury, NY) and Tissue Solutions (Glasgow, Scotland) (Table S4). Samples were embedded in 4% low-melting-point agarose. Once set, the tissue blocks were glued to a Leica VT1200s vibratome chuck and submerged in sterile PBS within the tissue reservoir. Tissue slices were prepared using the vibratome with the following settings: speed, 0.1 mm/s; amplitude, 0.7 mm; depth, 300 μm.

Slices were carefully placed on organotypic cell culture inserts within six-well tissue culture plates containing 1.1 mL of complete medium (RPMI 1640-10% fetal bovine serum [FBS]). The cultures were incubated on a rotating platform (55 rpm) for 1.5 h in a standard 37°C, 5% $CO_2$ incubator to acclimatize. Culture supernatant was then aspirated and replaced with fresh medium containing the indicated treatment. Cultures were incubated for 72 h as before. Every 24 h, 250 μL culture medium was sampled and replaced with warm, fresh medium.

Frozen DTCs were obtained from Discovery Life Sciences (Huntsville, AL) (Table S5). DTC samples were quickly thawed in a 37°C water bath and washed in 20 mL 1× CTL antiaggregate buffer (Thermo Fisher Scientific). Cells were plated in 96-well, round-bottomed plates at $1 \times 10^5$ cells per well in 50 μL of RPMI 1640 medium supplemented with 10% FBS. Cells were infected at an MOI of 1 and incubated for 72 h. Cultured supernatant was collected after 72 h to measure cytokines.

Culture supernatant from TSC was analyzed for the presence of human cytokines using a custom panel MSD-ECL assay (Meso Scale Discovery) detecting human IFN-α2a, IFN-γ, IL-1β, IL-6, IL-8, IL-10, IL-12p70, and tumor necrosis factor alpha (TNF-α). Assays were performed according to the manufacturer's instructions, and plates were read using a Meso Sector S 600 instrument (Meso Scale Discovery). Culture supernatants from DTCs were analyzed for the presence of cytokines, using a custom panel MSD-ECL (Meso Scale Discovery) for the detection of human IFN-α2a, IFN-γ, IL-10, IL-12p70, IL-1β, IL-2, IL-4, IL-6, IL-8, TNF-α, IFN-β, inflammatory protein-10, monocyte chemotactic protein-2, macrophage inflammatory protein-1α (MIP-1α), and MIP-1β. Assays were performed according to the manufacturer's instructions and plates were read with the Meso Sector S 600 instrument.

### Plaque assay

Vero cells were seeded the previous day at $3 \times 10^5$ cells per well per 0.5 mL in 24-well plates. Cell lysates and tissue homogenates were 10-fold serially diluted (from $10^{-1}$ to $10^{-7}$) in the Vero cell medium. Cell culture supernatants were then discarded, and 100 μL of each virus dilution was added to the cells and incubated at 37°C for 1 h. Two milliliters per well of Vero cell medium supplemented with methylcellulose (0.5%) was added and incubated for 48 or 72 h at 37°C with 5% $CO_2$ before staining with crystal violet. The plaques were counted, and the infectious titer was expressed in PFUs per milliliter, calculated with the following formula:

$$\text{Titer (PFU / mL)} = (\text{number of plaques}) \times (\text{dilution factor}) / (\text{inoculum volume})$$

### *In vivo* studies

Studies with PDX tumors were conducted at Crown Bioscience (San Diego, CA) in compliance with the US Department of Agriculture's Animal Welfare Act (9 CFR Parts 1, 2, and 3). Procedures involving the care and use of animals in this study were reviewed and approved by the Institutional Animal Care and Use Committee (IACUC) of CrownBio prior to execution and were conducted in accordance with the regulations of the Association for Assessment and Accreditation of Laboratory Animal Care (AAALAC).

To establish the 47 PDX models, cryo vials containing tumor cells were thawed and prepared for injection into mice. Thawed cells were washed in RPMI 1640 medium, counted, and resuspended in cold RPMI 1640 medium at a concentration of 50,000–100,000 viable cells per 50 μL. Cell suspensions were mixed with an equal volume of Cultrex extracellular matrix (ECM; R&D Systems, Minneapolis, MN) and kept on ice before implantation. Cells were prepared for injection by withdrawing ECM-cell mixture into a chilled 1-mL slip-tipped syringe. The filled syringes were kept on ice to avoid the solidification of ECM. Animals were shaved before injection. One mouse at a time was immobilized and the site of injection disinfected with an alcohol swab. One hundred milliliters of the cell suspension (50,000–100,000 cells) in ECM was subcutaneously injected into the rear flank of 9- to 29-week-old NOD-SCID mice.

For tumor chunk inoculation, frozen tumor fragments were thawed and cut into tumor chunks approximately 2–3 mm in diameter. Each mouse received a single injection of buprenorphine 30 min before tumor chunk implantation. One tumor chunk was loaded into a trocar needle and injected into the right front flank of each mouse for tumor development. Mice were ear tagged and left undisturbed for up to 7 days before being observed for tumor growth. Tumors were allowed to reach approximately 130–230 $mm^3$ before randomization. The antitumor effects of VACV-LUC were determined by comparing the growth curves for each treated tumor with that of a size-matched, untreated tumor. In this way, the BOR of the treated tumor compared to its size at the start of OV treatment (with progressive growth of the untreated tumor) was designated according to the following criteria: CR, no measurable tumor; PR, $\geq$30% decrease in tumor volume; DS, <30% decrease in tumor volume but <100% tumor volume increase sustained for at least 14 days after either the first or third dose; and PD, >100% increase in tumor volume. Tumors that did not fit into the categorization were considered nonevaluable.

All of the studies using human CDX or syngeneic mouse or rat tumors were conducted at AstraZeneca according to IACUC-approved protocols in the Laboratory Animal Resources facility at AstraZeneca, which is licensed by the AAALAC and the US Department of Agriculture.

Human CDXs were established by subcutaneous injection of $5 \times 10^6$ cells per 200 μL suspended in PBS into the right flank of 8- to 12-week-old NOD/SCID female mice. Mice were randomized into treatment groups of 10 animals each when tumor volumes reached 150–250 $mm^3$. The body weights of animals were monitored for welfare purposes and measured 2 times per week for 4 weeks, followed by once per week.

To establish MC38 and CT26 murine syngeneic tumor models for monotherapy and combination studies, cells were harvested and implanted by subcutaneous injection of $5 \times 10^5$ cells suspended in PBS into the right flanks of 7- to 9-week-old C57BL/6J (MC38) or 9- to 12-week-old Balb/c (CT26) female animals. Mice were randomized into treatment groups of 10 animals each when tumor volumes reached 150–250 $mm^3$. Mice body weights were monitored throughout the study. Some mice from the MC38 syngeneic mouse tumor study treated with monotherapy VACV control virus or VACV muIL-12 were euthanized before reaching tumor volume endpoints in the VACV control (3 mice) and VACV muIL-12 (4 mice) groups due to tumor ulceration. Tumor ulceration is most likely due to virus-mediated tumor destruction under the epidermis and can result in dermal infections if left untreated. For this reason, our IACUC protocol requires humane euthanasia for tumor ulceration. These events were included as endpoints for the purpose of Kaplan-Meier survival curve analysis. For combination studies with anti-mouse PD-L1 mAb, 10 mice per group were treated with intratumoral vehicle (PBS + 0.05% bovine serum albumin [BSA]), VACV-LUC control, or VACV muIL-12 viruses every 4 days for 3 doses. The next day after treatment with vehicle, VACV-LUC, or VACV muIL-12, the anti-mouse PD-L1 mAb clone 10F.9G2 (BioXCel Therapeutics, New Haven, CT) was administered at 10 mg/kg by intraperitoneal administration every 4 days for 4 doses. Tumors were collected at days 3 and 7 after the first VACV dose for dissociation of tumors for immunophenotyping of tumor-infiltrating lymphocytes.

To establish F98 tumors in Fischer 344 rats, cells were removed from flasks using trypsin solution before the neutralization of trypsin by adding DMEM and 10% FBS. Harvested cells were kept on ice from the time of harvest to implantation (not exceeding 3 h). Cells were injected by subcutaneous injection of $5.0 \times 10^6$ cells suspended in 0.2 mL of PBS into the right flanks of 7- to 9-week-old animals. Tumors were allowed to reach approximately 300–350 $mm^3$ before randomization.

### ELISpot assays

Single-cell suspensions were generated from the spleens of treated mice, followed by the lysis of red blood cells. A total of 250,000 cells per well were plated on IFN-γ ELISpot plates (catalog no. XEL485R&D; R&D Systems) and stimulated with a control peptide (LCMV gp33; New England Peptides, Gardner, MA) or the tumor-associated antigen AH-1 peptide (AnaSpec, Fremont, CA) (200 μg/mL) or VACV-associated antigen A52L (New England Peptides) (1 μg/mL). Cells were incubated for 48 h. Spots were visualized according to the manufacturer's protocol and counted using the S6 Universal M2 plate reader (ImmunoSpot, Shaker Heights, OH).

### *Ex vivo* analysis

To assess virus replication, mice were euthanized and blood, tumors, and normal tissues were collected and snap-frozen. Mouse plasma was prepared by high-speed centrifugation of EDTA anticoagulated whole blood (13,000 rpm for 10 min at 4°C in a table-top microcentrifuge). Frozen tumors and normal tissues were weighed and suspended in ice-cold homogenization buffer (PBS supplemented with 1× antibiotic-antimycotic [Thermo Fisher Scientific] and 1× Halt protease-phosphatase inhibitor [Thermo Fisher Scientific]) before being transferred to Matrix A tubes (MP Bio, Santa Ana, CA) and homogenized using the FastPrep-24 lysis system (MP Bio) for 20 s at 4 min per second. Tissue homogenates were then subjected to two freeze-thaw cycles, divided into aliquots, and stored at −80°C. Two additional aliquots that were not subjected to freeze thaws were prepared for virus recovery or cytokine analysis by MSD-ECL.

### Cytokine analysis

Aliquots from the tumor and spleen homogenates were centrifuged at 1,500 rpm for 5 min at 4°C. The supernatant was collected and stored at −80°C to measure cytokines. EDTA anticoagulated whole blood was collected from mice at the indicated time points, and mouse plasma was collected after centrifugation at 13,000 rpm for 10 min at 4°C and stored at −80°C. Plasma, tumor, and spleen lysates were diluted and measured using a murine or human IL-12p70 U-Plex MSD-ECL assay (Meso Scale Discovery), a custom U-Plex murine cytokine MSD-ECL assay (Meso Scale Discovery), or the immune monitoring 48-plex mouse ProcartaPlex Luminex panel (Thermo Fisher Scientific) according to the manufacturer's protocol.

### Tumor-infiltrating lymphocyte flow cytometry immunophenotyping analysis

Tumor tissues were digested using a tumor dissociation kit in the gentleMACS Octo Dissociator (Miltenyi Biotec, Auburn, CA). The resulting single-cell suspensions were filtered through a 70-μm cell strainer and washed in flow cytometry buffer (PBS + 2% FBS). For each sample, $1 \times 10^6$ cells were incubated with anti-mouse CD16/32 (BioLegend, San Diego, CA) to reduce nonspecific FcγR binding along with Live/Dead Fixable Blue viability dye (Thermo Fisher Scientific) at 1:1,000 for 30 min at 4°C. Cells were then bound to antibodies specific for cell surface immune markers in flow cytometry buffer for 30 min at 4°C followed by washes in cold flow cytometry buffer. These antibodies were CD45 BV785 (clone 30-F11; BioLegend), CD3- PE-Cy5 (clone 145-2C11; BioLegend), CD4-BUV395 (clone GK1.5; BD Biosciences), CD8-BUV737 (clone 53-6.7; BD Biosciences), CD69-BUV563 (clone H1.2F3; Biolegend), CD11c-BV480 (clone N418; BD Biosciences, Franklin Lakes, NJ), CD11b-BV650 (clone M1/70; BioLegend), PD-L1-APC (clone MIH5; BioLegend), Ly6c BV711 (clone HK1.4; BioLegend), and Ly6G BUV395 (clone 1A8; BioLegend). For identification of $FoxP3^+$ regulatory CD4 T cells, samples were fixed using the eBioscience Foxp3/Transcription kit (Invitrogen) for 45 min and subsequently incubated with Foxp3-APC (Clone FJK-16J, ThermoFisher Scientific) in permeabilization buffer for 45 min followed by washes in permeabilization buffer. Cells were analyzed on a Symphony A3 flow cytometer (BD Biosciences). Single stain controls (using cells or Ultracomp eBeads Plus; Thermo Fisher Scientific) and fluorescence minus one controls were analyzed in addition to the full immunophenotyping panel for proper fluorescence compensation and to define gating strategies. Approximately 500,000 events were counted for each sample to generate statistically robust data.

### Evaluation of antitumor and antivirus T cell immunity

Spleens were harvested from treated mice on day 7 after dosing and placed in fresh complete RPMI medium. Single-cell suspensions were generated by mechanical disruption and passed through a 70-mm filter. Red blood cells were lysed using 1× ACK lysis buffer (Thermo Fisher Scientific) for 5 min at room temperature and washed with complete RPMI medium. Single-cell splenocyte suspensions were plated at $2.5 \times 10^5$ cells/well in 100 mL complete RPMI medium supplemented with 1× antibiotic-antimycotic in IFN-γ ELISpot plates (R&D Systems). Peptides (control, A52L, and AH1) were prepared and added to splenocytes at 1 mg/mL. Untreated and phorbol 12-myristate 13-acetate (0.25 μg/mL)/ionomycin (1 mg/mL) controls were also prepared. Stimulated splenocytes were incubated for 48 h, and IFN-γ-secreting cells were visualized using the IFN-γ ELISpot kit (R&D Systems) according to the manufacturer's protocol. Spots were visualized and quantified using an ELISA plate reader (ImmunoSpot).

### IFN-γ competitive ELISA

Recombinant rat IFN-γ (1 ng/mL) (R&D Systems) was mixed with PBS, recombinant B8R (50 ng/mL) (R&D Systems), or 0.2-μm-filtered supernatant from HeLa cells infected with AZD4820 (1 MOI) and incubated at 37°C for 1 h. Since B8R binds IFN-γ and prevents antibodies from detection by ELISA, we next performed an ELISA to determine the percent recovery of IFN-γ, as described below. Percent recovery was calculated relative to IFN-γ alone.

### ELISAs

Rat IFN-γ was measured in the plasma of rats treated with VACV at the indicated time points. Plasma was diluted and IFN-γ was measured using the Rat IFN-γ DuoSet Elisa (R&D Systems) according to the manufacturer's protocol.

### IHC

The tissues were trimmed, fixed in neutral buffered formalin, and stored in 70% ethanol. They were then processed through graded

ethanol (70%, 95%, 100%), cleared with xylene, and infiltrated with paraffin. Tissue samples were combined (kidney and liver; ovary and xenograft; lung and spleen), embedded in paraffin blocks, and sectioned at 4-μm thickness before being collected onto Starfrost glass microscope slides (MER 7255; Mercedes Scientific, Lakewood Ranch, FL). Samples were stained for VACV on a Ventana Discovery autostainer with the following protocol: 4-min enzyme digestion with Protease (760–2018; Roche Diagnostics, Indianapolis, IN) at 35°C, 12-min endogenous peroxide blocking (760-159; Roche), 40-min incubation with primary anti-VACV polyclonal rabbit antibody (ab117453, diluted to 5.3 μg/mL; Abcam, Cambridge, UK) at 37°C, 20-min incubation with OmniMap anti-rabbit horseradish peroxidase secondary antibody (760-4311; Roche), development with diaminobenzidine, 12-min counterstain in hematoxylin (790-2208; Roche) and Bluing Reagent (760-2037; Roche). The rabbit polyclonal anti–vaccinia virus primary antibody ab117453 targets the fusion protein A27L.

#### Statistical analysis

The difference between virus recovered from human PDX tumors after the first or third dose of VACV-LUC was determined by two-tailed, paired Student t test, using Prism software, version 9.0.0 (GraphPad Software, San Diego, CA). Differences in gene expression from human PDX tumor samples grouped according to patterns of response to VACV-LUC were determined by one-way ANOVA with Kruskal-Wallis test for multiple comparisons, using Prism software. The correlation between the *in vitro* oncolytic activity of VACV IL-12 (AZD4820) and VACV-LUC across human tumor cell lines was assessed with linear regression analysis followed by the determination of Pearson correlation coefficient and associated p value with Prism software. Differences in tumor volume of human tumor cell lines engrafted in immunodeficient mice at indicated times during an experiment were assessed using one-way ANOVA with Tukey correction for multiple comparisons with Prism software. One-way ANOVA with Tukey correction for multiple comparisons was also used to assess differences between cytokine and mRNA levels detected in primary human TSC and DTC samples, as well as to determine the statistical significance of differences in antitumor activity at day 18, PD-L1$^+$ cell populations, and ELISpot spot-forming units after splenocyte peptide stimulation in the anti-mouse PD-L1 combination studies using the CT26 model. Statistical analyses of differences in peripheral cytokine levels in the plasma of CT26 or MC38 tumor-engrafted mice treated with VACV muIL-12 were performed on log transformed data and analyzed by Kruskal-Wallis test and Dunn multiple comparisons test. Differences in median survival in CT26 and MC38 studies were performed using a log rank test in Prism software.

## DATA AND CODE AVAILABILITY

Data underlying the findings described in this paper may be obtained in accordance with AstraZeneca's data sharing policy described at https://astrazenecagrouptrials.pharmacm.com/ST/Submission/Disclosure.

## SUPPLEMENTAL INFORMATION

Supplemental information can be found online at https://doi.org/10.1016/j.omton.2023.200758.

## ACKNOWLEDGMENTS

We thank Noel Monks, Ivan Inigo, Viviana Taylor, Morgan Kink, Manish Neupane, Leigh Hostetler, Keegan Loveless, Mel Ehudin, Pan, Ravinder Tammali, Jon Chesebrough, and Kim Cook at AstraZeneca for support with the *in vivo* and *in vitro* studies. We also thank Anna Huntley and Kim Maratea at AstraZeneca for conducting the histological analysis. Finally, we would like to recognize our partners at Crown Bioscience (San Diego, CA) for conducting antitumor efficacy studies in PDX models and those patients who consented for their tumor tissues to be used in preclinical research. This study was funded solely by AstraZeneca and Transgene SA.

## AUTHOR CONTRIBUTIONS

Conception and design: C.K., S.A., A.M., E.G., S.B., N.R.M., J.F., E.Q., N.S., P.S., C.B., S.A.H., E.J.K., J.L., N.M.D., M.O., and M.A.S.B.; collection and assembly of data: C.K., S.A., A.M., E.G., S.B., A.V., R.R., K.S., N.R.M., N.S., C.D., P.K., M.O., and M.A.S.B.; data analysis and interpretation: C.K., S.A., A.M., E.G., S.B., R.R., K.S., J.F., M.O., and M.A.S.B.; manuscript writing: C.K., S.A., A.M., E.G., S.B., M.O., and M.A.S.B.; all of the authors approved the final version of the manuscript.

## DECLARATION OF INTERESTS

At the time this study was conducted, C.K., S.A., A.M., E.G., S.B., A.V., R.R., K.S., N.R.M., P.S., C.B., S.A.H., E.J.K., J.L., N.M.D., M.O., and M.A.S.B. were employees of AstraZeneca, with stock ownership and/or stock options or interests in the company; and J.F., N.S., E.Q., C.D., and P.K. were employees and stockholders of Transgene SA. N.R.M is an employee of Ratio Therapeutics (Boston, MA).

## REFERENCES

1. Galanis, E., Hartmann, L.C., Cliby, W.A., Long, H.J., Peethambaram, P.P., Barrette, B.A., Kaur, J.S., Haluska, P.J., Jr., Aderca, I., Zollman, P.J., et al. (2010). Phase I trial of intraperitoneal administration of an oncolytic measles virus strain engineered to express carcinoembryonic antigen for recurrent ovarian cancer. Cancer Res. *70*, 875–882.

2. Kaufman, H.L., Kim, D.W., DeRaffele, G., Mitcham, J., Coffin, R.S., and Kim-Schulze, S. (2010). Local and distant immunity induced by intralesional vaccination with an oncolytic herpes virus encoding GM-CSF in patients with stage IIIc and IV melanoma. Ann. Surg Oncol. *17*, 718–730.

3. Kurokawa, C., Iankov, I.D., Anderson, S.K., Aderca, I., Leontovich, A.A., Maurer, M.J., Oberg, A.L., Schroeder, M.A., Giannini, C., Greiner, S.M., et al. (2018). Constitutive interferon pathway activation in tumors as an efficacy determinant following oncolytic virotherapy. J. Natl. Cancer Inst. *110*, 1123–1132.

4. Heo, J., Reid, T., Ruo, L., Breitbach, C.J., Rose, S., Bloomston, M., Cho, M., Lim, H.Y., Chung, H.C., Kim, C.W., et al. (2013). Randomized dose-finding clinical trial of oncolytic immunotherapeutic vaccinia JX-594 in liver cancer. Nat. Med. *19*, 329–336.

5. Alcamí, A., and Smith, G.L. (1995). Vaccinia, cowpox, and camelpox viruses encode soluble gamma interferon receptors with novel broad species specificity. J. Virol. *69*, 4633–4639.

6. Andtbacka, R.H.I., Kaufman, H.L., Collichio, F., Amatruda, T., Senzer, N., Chesney, J., Delman, K.A., Spitler, L.E., Puzanov, I., Agarwala, S.S., et al. (2015). Talimogene

laherparepvec improves durable response rate in patients with advanced melanoma. J. Clin. Oncol. *33*, 2780–2788.

7. Zheng, M., Huang, J., Tong, A., and Yang, H. (2019). Oncolytic viruses for cancer therapy: barriers and recent advances. Mol. Ther. Oncolytics *15*, 234–247.
8. Breitbach, C.J., Burke, J., Jonker, D., Stephenson, J., Haas, A.R., Chow, L.Q.M., Nieva, J., Hwang, T.H., Moon, A., Patt, R., et al. (2011). Intravenous delivery of a multi-mechanistic cancer-targeted oncolytic poxvirus in humans. Nature *477*, 99–102.
9. Foloppe, J., Kempf, J., Futin, N., Kintz, J., Cordier, P., Pichon, C., Findeli, A., Vorburger, F., Quemeneur, E., and Erbs, P. (2019). The enhanced tumor specificity of TG6002, an armed oncolytic vaccinia virus deleted in two genes involved in nucleotide metabolism. Mol. Ther. Oncolytics *14*, 1–14.
10. Roberts, K.L., and Smith, G.L. (2008). Vaccinia virus morphogenesis and dissemination. Trends Microbiol. *16*, 472–479.
11. Appleyard, G., Hapel, A.J., and Boulter, E.A. (1971). An antigenic difference between intracellular and extracellular rabbitpox virus. J. Gen. Virol. *13*, 9–17.
12. Vanderplasschen, A., Mathew, E., Hollinshead, M., Sim, R.B., and Smith, G.L. (1998). Extracellular enveloped vaccinia virus is resistant to complement because of incorporation of host complement control proteins into its envelope. Proc. Natl. Acad. Sci. USA *95*, 7544–7549.
13. Vanderplasschen, A., Hollinshead, M., and Smith, G.L. (1997). Antibodies against vaccinia virus do not neutralize extracellular enveloped virus but prevent virus release from infected cells and comet formation. J. Gen. Virol. *78* (Pt 8), 2041–2048.
14. Smith, G.L., Benfield, C.T.O., Maluquer de Motes, C., Mazzon, M., Ember, S.W.J., Ferguson, B.J., and Sumner, R.P. (2013). Vaccinia virus immune evasion: mechanisms, virulence and immunogenicity. J. Gen. Virol. *94*, 2367–2392.
15. Walsh, S.R., and Dolin, R. (2011). Vaccinia viruses: vaccines against smallpox and vectors against infectious diseases and tumors. Expert Rev. Vaccines *10*, 1221–1240.
16. Kaufman, H.L., Kohlhapp, F.J., and Zloza, A. (2015). Oncolytic viruses: a new class of immunotherapy drugs. Nat. Rev. Drug Discov. *14*, 642–662.
17. Kirn, D.H., and Thorne, S.H. (2009). Targeted and armed oncolytic poxviruses: a novel multi-mechanistic therapeutic class for cancer. Nat. Rev. Cancer *9*, 64–71.
18. Thorne, S.H. (2014). Immunotherapeutic potential of oncolytic vaccinia virus. Front. Oncol. *4*, 155.
19. Chiocca, E.A., and Rabkin, S.D. (2014). Oncolytic viruses and their application to cancer immunotherapy. Cancer Immunol. Res. *2*, 295–300.
20. Watford, W.T., Moriguchi, M., Morinobu, A., and O'Shea, J.J. (2003). The biology of IL-12: coordinating innate and adaptive immune responses. Cytokine Growth Factor Rev. *14*, 361–368.
21. Tugues, S., Burkhard, S.H., Ohs, I., Vrohlings, M., Nussbaum, K., Vom Berg, J., Kulig, P., and Becher, B. (2015). New insights into IL-12-mediated tumor suppression. Cell Death Differ. *22*, 237–246.
22. Nguyen, K.G., Vrabel, M.R., Mantooth, S.M., Hopkins, J.J., Wagner, E.S., Gabaldon, T.A., and Zaharoff, D.A. (2020). Localized interleukin-12 for cancer immunotherapy. Front. Immunol. *11*, 575597.
23. Atkins, M.B., Robertson, M.J., Gordon, M., Lotze, M.T., DeCoste, M., DuBois, J.S., Ritz, J., Sandler, A.B., Edington, H.D., Garzone, P.D., et al. (1997). Phase I evaluation of intravenous recombinant human interleukin 12 in patients with advanced malignancies. Clin. Cancer Res. *3*, 409–417.
24. Johnson, D.B., Nebhan, C.A., Moslehi, J.J., and Balko, J.M. (2022). Immune-checkpoint inhibitors: long-term implications of toxicity. Nat. Rev. Clin. Oncol. *19*, 254–267.
25. Harrington, K.J., Kong, A., Mach, N., Chesney, J.A., Fernandez, B.C., Rischin, D., Cohen, E.E.W., Radcliffe, H.S., Gumuscu, B., Cheng, J., et al. (2020). Talimogene laherparepvec and pembrolizumab in recurrent or metastatic squamous cell carcinoma of the head and neck (MASTERKEY-232): a multicenter, phase 1b study. Clin. Cancer Res. *26*, 5153–5161.
26. Panagioti, E., Kurokawa, C., Viker, K., Ammayappan, A., Anderson, S.K., Sotiriou, S., Chatzopoulos, K., Ayasoufi, K., Johnson, A.J., Iankov, I.D., and Galanis, E. (2021). Immunostimulatory bacterial antigen-armed oncolytic measles virotherapy significantly increases the potency of anti-PD1 checkpoint therapy. J. Clin. Invest. *131*, e141614.
27. Liu, B., Song, Y., and Liu, D. (2017). Recent development in clinical applications of PD-1 and PD-L1 antibodies for cancer immunotherapy. J. Hematol. Oncol. *10*, 174.
28. Shultz, L.D., Schweitzer, P.A., Christianson, S.W., Gott, B., Schweitzer, I.B., Tennent, B., McKenna, S., Mobraaten, L., Rajan, T.V., Greiner, D.L., et al. (1995). Multiple defects in innate and adaptive immunologic function in NOD/LtSz-scid mice. J. Immunol. *154*, 180–191.
29. Shultz, L.D., Lyons, B.L., Burzenski, L.M., Gott, B., Chen, X., Chaleff, S., Kotb, M., Gillies, S.D., King, M., Mangada, J., et al. (2005). Human lymphoid and myeloid cell development in NOD/LtSz-scid IL2R gamma null mice engrafted with mobilized human hemopoietic stem cells. J. Immunol. *174*, 6477–6489.
30. Schoenhaut, D.S., Chua, A.O., Wolitzky, A.G., Quinn, P.M., Dwyer, C.M., McComas, W., Familletti, P.C., Gately, M.K., and Gubler, U. (1992). Cloning and expression of murine IL-12. J. Immunol. *148*, 3433–3440.
31. Segal, J.G., Lee, N.C., Tsung, Y.L., Norton, J.A., and Tsung, K. (2002). The role of IFN-gamma in rejection of established tumors by IL-12: source of production and target. Cancer Res. *62*, 4696–4703.
32. Okura, Y., Takeda, K., Honda, S., Hanawa, H., Watanabe, H., Kodama, M., Izumi, T., Aizawa, Y., Seki, S., and Abo, T. (1998). Recombinant murine interleukin-12 facilitates induction of cardiac myosin-specific type 1 helper T cells in rats. Circ. Res. *82*, 1035–1042.
33. Guo, Z.S., Lu, B., Guo, Z., Giehl, E., Feist, M., Dai, E., Liu, W., Storkus, W.J., He, Y., Liu, Z., and Bartlett, D.L. (2019). Vaccinia virus-mediated cancer immunotherapy: cancer vaccines and oncolytics. J. Immunother. Cancer *7*, 6.
34. Chon, H.J., Lee, W.S., Yang, H., Kong, S.J., Lee, N.K., Moon, E.S., Choi, J., Han, E.C., Kim, J.H., Ahn, J.B., et al. (2019). Tumor microenvironment remodeling by intratumoral oncolytic vaccinia virus enhances the efficacy of immune-checkpoint blockade. Clin. Cancer Res. *25*, 1612–1623.
35. Nakao, S., Arai, Y., Tasaki, M., Yamashita, M., Murakami, R., Kawase, T., Amino, N., Nakatake, M., Kurosaki, H., Mori, M., et al. (2020). Intratumoral expression of IL-7 and IL-12 using an oncolytic virus increases systemic sensitivity to immune checkpoint blockade. Sci. Transl. Med. *12*, eaax7992.
36. Chen, X., Tao, Y., He, M., Deng, M., Guo, R., Sheng, Q., Wang, X., Ren, K., Li, T., He, X., et al. (2021). Co-delivery of autophagy inhibitor and gemcitabine using a pH-activatable core-shell nanobomb inhibits pancreatic cancer progression and metastasis. Theranostics *11*, 8692–8705.
37. Kim, M.K., Breitbach, C.J., Moon, A., Heo, J., Lee, Y.K., Cho, M., Lee, J.W., Kim, S.G., Kang, D.H., Bell, J.C., et al. (2013). Oncolytic and immunotherapeutic vaccinia induces antibody-mediated complement-dependent cancer cell lysis in humans. Sci. Transl. Med. *5*, 185ra63.
38. Rojas, J.J., Sampath, P., Hou, W., and Thorne, S.H. (2015). Defining effective combinations of immune checkpoint blockade and oncolytic virotherapy. Clin. Cancer Res. *21*, 5543–5551.
39. Rivadeneira, D.B., DePeaux, K., Wang, Y., Kulkarni, A., Tabib, T., Menk, A.V., Sampath, P., Lafyatis, R., Ferris, R.L., Sarkar, S.N., et al. (2019). Oncolytic viruses engineered to enforce leptin expression reprogram tumor-infiltrating T cell metabolism and promote tumor clearance. Immunity *51*, 548–560.e4.
40. Kaufman, H.L., Flanagan, K., Lee, C.S.D., Perretta, D.J., and Horig, H. (2002). Insertion of interleukin-2 (IL-2) and interleukin-12 (IL-12) genes into vaccinia virus results in effective anti-tumor responses without toxicity. Vaccine *20*, 1862–1869.
41. Ge, Y., Wang, H., Ren, J., Liu, W., Chen, L., Chen, H., Ye, J., Dai, E., Ma, C., Ju, S., et al. (2020). Oncolytic vaccinia virus delivering tethered IL-12 enhances antitumor effects with improved safety. J. Immunother. Cancer *8*, e000710.
42. Mastrangelo, M.J., Maguire, H.C., Jr., Eisenlohr, L.C., Laughlin, C.E., Monken, C.E., McCue, P.A., Kovatich, A.J., and Lattime, E.C. (1999). Intratumoral recombinant GM-CSF-encoding virus as gene therapy in patients with cutaneous melanoma. Cancer Gene Ther. *6*, 409–422.
43. Foloppe, J., Kintz, J., Futin, N., Findeli, A., Cordier, P., Schlesinger, Y., Hoffmann, C., Tosch, C., Balloul, J.M., and Erbs, P. (2008). Targeted delivery of a suicide gene to human colorectal tumors by a conditionally replicating vaccinia virus. Gene Ther. *15*, 1361–1371.